# Actuator Stiction Compensation via Model Predictive Control for Nonlinear Processes

**Helen Durand**
Dept. of Chemical and Biomolecular Engineering, University of California, Los Angeles, CA 90095-1592

**Panagiotis D. Christofides**
Dept. of Chemical and Biomolecular Engineering, University of California, Los Angeles, CA 90095-1592

Dept. of Electrical Engineering, University of California, Los Angeles, CA 90095-1592

*DOI 10.1002/aic.15171*
*Published online February 13, 2016 in Wiley Online Library (wileyonlinelibrary.com)*

*The problem of valve stiction is addressed, which is a nonlinear friction phenomenon that causes poor performance of control loops in the process industries. A model predictive control (MPC) stiction compensation formulation is developed including detailed dynamics for a sticky valve and additional constraints on the input rate of change and actuation magnitude to reduce control loop performance degradation and to prevent the MPC from requesting physically unrealistic control actions due to stiction. Although developed with a focus on stiction, the MPC-based compensation method presented is general and has potential to compensate for other nonlinear valve dynamics which have some similarities to those caused by stiction. Feasibility and closed-loop stability of the proposed MPC formulation are proven for a sufficiently small sampling period when Lyapunov-based constraints are incorporated. Using a chemical process example with an economic model predictive controller (EMPC), the selection of appropriate constraints for the proposed method is demonstrated. The example verified the incorporation of the stiction dynamics and actuation magnitude constraints in the EMPC causes it to select set-points that the valve output can reach and causes the operating constraints to be met.*
 *AIChE J*, 62: 2004–2023, 2016
*Keywords: model predictive control, valve dynamics, chemical processes, process control, economic model predictive control, stiction*

## Introduction

Model predictive control (MPC) is a popular optimization-based control method in the chemical process industries and as a result, has received extensive academic research attention, with many variants developed to address the range of goals that industry may have. A commonality between all of the MPC strategies is that they require a sufficiently accurate process model for good performance. This process model should include significant dynamics of the process, including those of the valves if they cannot be assumed to be instantaneous. However, although valve dynamics, particularly nonlinear valve dynamics such as stiction and backlash, often cause poor performance of control loops in industry,[1,2] valve dynamics are seldom incorporated in developments in MPC.

Valve stiction is a phenomenon caused by friction between valve components and refers to the tendency of a valve not to move upon the change of the control signal sent to the valve until the control signal exceeds a certain threshold, at which time there may be a sudden movement of the valve components causing the valve output (i.e., process manipulated input) to change quickly. The percentage of the available range of valve outputs traversed when the valve output changes quickly quantifies the phenomenon of slip-jump. When the valve is moving (in the moving phase), the valve output typically is linearly related to the valve input until the changes in the valve input change sign (i.e., the valve input begins to decrease when it was previously increasing, or vice versa), at which point the valve begins to stick again. Because stiction has been characterized in various ways by different authors, the authors of Ref. 3 compile some of the stiction definitions, ending with the definition determined by the authors based on observations of plant data, which classifies stiction as a friction effect that manifests itself through a sudden change in the valve output in response to a changing input signal. Specifically, the authors of Ref. 3 define four major regimes in the dynamic response of the control valve output to changes in the input to the valve determined by the controller: deadband, stickband, slip-jump, and the moving phase. In the absence of slip-jump, only deadband (i.e., the percentage of the available range of the input signals to the valve throughout which the valve output does not change in the absence of slip-jump) and the moving phase exist. When a valve experiences slip-jump, the valve remains stuck throughout the deadband and also throughout a percentage of the available range of inputs beyond the deadband (called the stickband) until it slips from the value at which it was stuck to a value in the moving phase.

Correspondence concerning this article should be addressed to P. D. Christofides at pdc@seas.ucla.edu.

Stiction has posed a significant issue in chemical process control throughout the last several decades. Reports from the 1990s indicated that stiction negatively affected control loop performance at the time,[4,5] and a report from Honeywell indicated that when studying 26,000 proportional-integral-derivative (PID) controllers, the performance of about one-third was classified in the lowest of the classification categories ("poor" and "fair"), with valve issues, including stiction, causing about one-third of these low classifications.[1] More recently, Ref. 6 cited stiction as a contributor to plantwide oscillations and included plant data from the Mitsubishi Chemical Corporation for a plant where stiction contributed to plantwide oscillations. In addition, in Ref. 7, the proposed stiction detection and quantification method is performed on industrial data for plants with sticky valves, demonstrating that the problem of valve stiction remains a challenging one. As a result, a significant level of research has been performed throughout the years in an attempt to more accurately model, detect, quantify, and combat stiction (see the review paper Ref. 8 for a general overview of stiction modeling, detection, quantification, and compensation).

The physical cause of stiction in control valves is best explained using a specific valve type for clarity of presentation, but the same basic principles will hold for other valve types as well. For example, a pneumatic spring-diaphragm sliding-stem globe valve has a valve stem that, in response to a pressure applied to a diaphragm, moves to adjust the valve output. In a valve with stiction, the valve output may not approach the value requested due to friction forces between the valve stem and the packing that can prevent the valve stem from moving to the required position until the pressure applied to the valve diaphragm is large enough to overcome the breakaway force for the packing-stem contact. The cause of friction between the valve stem and the packing is that the materials from which the stem and packing are made are rough at a microscopic level, with protrusions called asperities. The interactions of the asperities on the two surfaces result in friction forces.[9] The friction phenomenon is often described using static, Coulomb, and viscous friction, as well as the Stribeck effect. However, there are a number of other phenomena that result from friction, including rising static friction, presliding displacement (microslip), frictional memory in sliding, stick-slip,[9] hysteresis with nonlocal memory during presliding,[10] velocity weakening, the lift-up effect,[11] and asymmetric stiction.[12]

Friction models have been developed throughout the years that model these friction effects to varying degrees. For example, the Classical[4,13] model only accounts for the Coulomb and viscous forces and the Stribeck effect in the sliding regime, representing any presliding dynamics with a static friction force. As models were developed throughout time, such as the Dahl,[14,15] LuGre,[16] Leuven,[10,17] Elasto-Plastic,[18] and generalized Maxwell-Slip[19] models, they began to incorporate some of the more subtle friction effects in both the presliding and sliding regimes. A generic model that attempted to represent the known friction dynamics by modeling various interactions between asperities was also developed.[11] A number of researchers have also developed algorithm-based empirical friction models, known as data-driven models, that attempt to represent friction dynamics using decision tree structures. This class of models includes the Stenman,[20] Choudhury,[3] Kano,[21] and He[22] models.

A number of works utilizing friction models in control strategies to counter friction have examined adapting friction model parameters.[23–25] In addition, the parameters of the friction model change with time for a valve as stiction worsens over time, which may occur for reasons such as tightening of the valve packing or degradation or depletion of materials that comprise or lubricate the valve.[26,27] For example, in Refs. 4 and 5, it is seen that as stiction worsens in a pneumatic sliding-stem globe valve, the range of stem positions that can be reached with a given range of pressures applied to the valve is reduced. This is significant because the pressure available to be applied to a valve is limited,[28] with the result that as stiction worsens, the given range of pressures cannot move the valve stem as significantly as when stiction was minimal. This shows that a negative effect of stiction is that it changes the valve dynamics and in effect constrains the range of valve outputs available for a given range of actuation magnitudes.

Other negative effects of stiction include set-point tracking issues and oscillations in control loops that result from deadband/stickband and slip-jump. For example, when a valve has deadband/stickband, the valve output does not change in response to changes in the control signal to the valve until the control signal overcomes the deadband/stickband, which prevents the valve output from tracking its set-point. Oscillations can occur in a control loop with integral action and a valve with deadband/stickband and slip-jump due to effects similar to those caused by wind-up in an integrating controller. If there is significant deadband/stickband before the valve slips and the valve controller is aggressive, the integral action becomes large, and although it may be desirable to stop the valve from moving or to move it in the opposite direction soon after it slips, the integral action of the controller causes it to continue moving in the original direction for some time, resulting in overshoot of the set-point and possibly oscillations as occurs in the case of controller wind-up.[29] In addition, slip-jump is known to contribute to oscillatory behavior.[7]

A good deal of work has been performed to reduce the negative effects of stiction on engineering processes. As mentioned above with respect to adapting friction model parameters, a number of methods have been developed to reduce the tracking offset that can result from friction (many appear in the literature for high-precision mechanical applications such as machining) using control laws based on a friction model (see, e.g., Refs. 5 and 30). Much of the stiction compensation literature for sticky valves in chemical plant control loops has focused on reducing oscillations. Methods for oscillation reduction include the knocker and variations upon it[26,27,31,32] and the constant reinforcement method of Ref. 29, which add signals to the controller output to reduce the amplitude of oscillations in the process variable that is controlled by manipulating the valve output. Other methods include the two moves method and its extensions,[33–35] which attempt to drive the valve stem to a specific position, an optimization method[33] which can compute compensating signals to add to controller outputs to minimize undesirable effects of stiction compensation such as excessive stem movement, and retuning methods.[36–38]

An observation is that the stiction compensation literature for oscillating control loops often refers to processes in which the process variable controlled by the valve output is measured and fed back to a controller. Because the deadband/stickband may cause the valve dynamics to act like a time delay in the control loop in such a case, and time delays in a control loop are known to cause oscillations, this effect may contribute to the oscillations observed in some cases; however, although the control architecture used to control a sticky valve may have an impact in some cases on the poor performance of a control

loop, it can often be the deadband/stickband combined with slip-jump, rather than the control architecture, that causes the limit cycle behavior observed in numerous control loops containing sticky valves.

In addition to the stiction compensation methods mentioned above, predictive control methods have also been looked at for stiction compensation. In Ref. 39, a predictive controller for applications requiring high precision of mechanical movement was augmented by time delay control and zero phase error tracking control to improve its tracking performance in the presence of nonlinear friction effects. Nonlinear MPC is used in Ref. 40 to control a hydraulic actuator subject to constraints. In Ref. 41, MPC and a deadzone compensator are used to control a gantry crane subject to deadzone and saturation. In Ref. 42, an inverse backlash model and valve saturation are incorporated in an MPC for linear systems to overcome the deadband associated with backlash, and this controller is applied to a system with stiction in Ref. 43. In Ref. 44, the bounds on the optimization variables computed by an MPC are adjusted based on the knowledge that the MPC is in series with a unit that applies the inverse model for deadzone, stiction, or backlash to the output from the MPC and sends this signal to a valve with nonlinear dynamics that can saturate.

In this work, we propose MPC incorporating stiction dynamics, actuation magnitude constraints, and input rate of change constraints as a stiction compensation strategy for nonlinear process systems. We use a control architecture that avoids potential oscillation issues caused by delays in control loops and develop a process-valve dynamic model to be incorporated in MPC that includes detailed dynamics for a valve with stiction. We suggest a number of variations to the cost function and constraints of the proposed MPC such that it can be formulated to alleviate set-point tracking errors and oscillations due to stiction for a variety of cases. We further elucidate the need for actuation magnitude constraints in the proposed MPC to ensure that the set-points calculated by the controller remain physically reachable as stiction worsens. With the addition of Lyapunov-based stability constraints and a sufficiently small sampling period, the proposed controller is proven to be recursively feasible and to ensure closed-loop stability of the nonlinear process-valve system. Through a chemical process example, we motivate the addition of actuation magnitude constraints to MPC for stiction compensation and demonstrate the improvement in the set-point tracking ability of valves when the actuator dynamics and actuation magnitude constraints are incorporated in MPC compared to the case when they are not. The focus of the discussion is on compensating for stiction in control loops; however, the proposed method is flexible and could be examined as a compensating strategy for other valve nonlinearities as well. Although the technique of incorporating valve dynamics in MPC to improve control performance is similar to the approach in Ref. 45, which demonstrated that for a linear actuator layer, the incorporation of actuator dynamics in economic model predictive control (EMPC) can be important for ensuring that process constraints are satisfied, this work significantly extends the concepts of that work to compensate directly for the nonlinear dynamics of stiction. Specifically, it develops additional constraints that should be considered for use in MPC when valves are known to have stiction in order to compensate for its effects, and the results impact all variants of MPC, rather than EMPC only.

## Preliminaries

### Notation

In this work, $t_k = k\Delta$, $k = 0, 1, 2, \ldots$ refers to synchronous time instants separated by a sampling period $\Delta$. The Euclidean norm of a vector is denoted by $|\cdot|$. A function $\alpha : [0, a) \rightarrow [0, \infty)$ with $\alpha(0) = 0$ belongs to class $\mathcal{K}$ if it is continuous and strictly increasing. A level set of a scalar-valued positive definite function $V(x)$ is defined to be the set $\Omega_\rho := \{x \in R^n \,|\, V(x) \leq \rho\}$. Set subtraction is denoted using "/" (i.e., $x \in A/B := \{x \in R^n \,|\, x \in A,\ x \notin B\}$).

### Class of systems

In this work, we develop a process-valve model for use in MPC that incorporates the dynamics of the process as well as the dynamics of the valves. This model includes dynamic equations for the process, the valve position, the valve output, and a linear controller for the valve. We introduce these equations separately, and then present the integrated model that combines them.

*Class of nonlinear processes.* We consider nonlinear processes of the form

$$\dot{x} = f(x(t), u_a(t), w(t)) \tag{1}$$

where $x \in R^n$, $u_a \in R^m$, and $w \in R^w$ are vectors of the process states, process inputs, and process disturbances, respectively. The inputs $u_a$ to the process are the outputs from the valves, which will be further detailed below. Due to the physical limitations on the valve opening, we assume that each input $u_{a,i}$, $i = 1, \ldots, m$, to the process is bounded within $U_i$ ($U_i := \{u_{a,i} | u_{a,i,\min} \leq u_{a,i} \leq u_{a,i,\max}\}$). We also assume that the disturbance is bounded ($w \in W := \{w | \, |w| \leq \theta, \theta > 0\}$). We note that the model of Eq. 1 can be constructed either through first-principles or system identification techniques.

*Nonlinear valve dynamics.* Using a force balance on the valve moving parts, we describe the valve dynamics by $x_{v,i}$ and $v_{v,i}$, which are variables representative of the position and velocity of the moving parts of the $i$th valve relative to the valve surfaces causing friction. The differential equations for these two variables are

$$\frac{dx_{v,i}}{dt} = v_{v,i} \tag{2}$$

$$\frac{dv_{v,i}}{dt} = \frac{1}{m_{v,i}}[c_i^T F_{O,i} - F_{f,i} - b_i^T F_{I,i}] \tag{3}$$

where $m_{v,i}$ is the mass of the moving parts that experience friction for the $i$th valve, $F_{O,i} \in R^{p_i}$ is a vector of forces acting on the valve in the direction opposite friction, $F_{f,i}$ is the friction force on the $i$th valve, and $F_{I,i} \in R^{s_i}$ is a vector of nonfriction forces acting on the valve in the same direction as the friction force. The vectors $c_i \in R^{p_i}$ and $b_i \in R^{s_i}$ are vectors of coefficients of the forces that are components of $F_{O,i}$ and $F_{I,i}$. The friction force $F_{f,i}$ experienced by the valve moving parts causes the effects referred to as stiction, and can be described by a general nonlinear model that is a function of $x_{v,i}$, $v_{v,i}$, and internal state variables $z_{f,i} \in R^{z_i}$ of the friction model as follows

$$F_{f,i} = \hat{F}_{f,i}(x_{v,i}, v_{v,i}, z_{f,i}) \tag{4}$$

$$\dot{z}_{f,i} = \hat{z}_{f,i}(x_{v,i}, v_{v,i}, z_{f,i}) \tag{5}$$

where $\hat{F}_{f,i}$ and $\hat{z}_{f,i}$ are nonlinear functions describing the friction force and the dynamics of the friction model states.

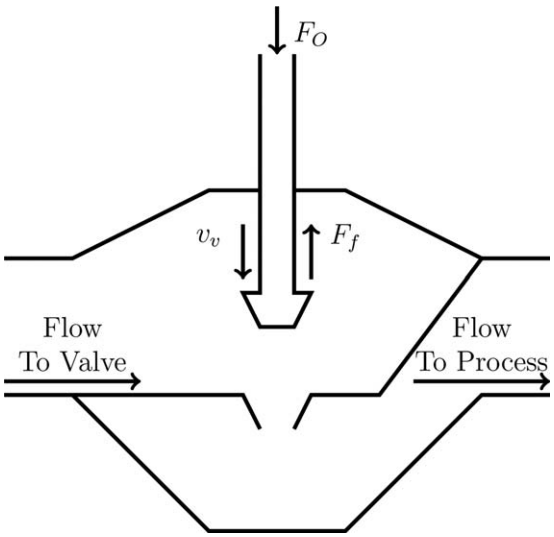


**Figure 1. Schematic of forces on an example valve.**

Assuming that each valve controls one process input, we define the three state vectors $x_v=[x_{v,1}\ \dots\ x_{v,m}]^T$, $v_v=[v_{v,1}\ \dots\ v_{v,m}]^T$, and $z_f=[z_{f,1}^T\ \dots\ z_{f,m}^T]^T$, as well as the vectors related to nonfriction forces acting on the valve, $c=[c_1^T\ \dots\ c_m^T]^T$, $F_O=[F_{O,1}^T\ \dots\ F_{O,m}^T]^T$, $b=[b_1^T\ \dots\ b_m^T]^T$, and $F_I=[F_{I,1}^T\ \dots\ F_{I,m}^T]^T$. For simplicity of notation, we define $\hat{v}_v=[\hat{v}_{v,1}\ \dots\ \hat{v}_{v,m}]^T$, where $\hat{v}_{v,i}=\hat{v}_{v,i}(c_i,F_{O,i},b_i,F_{I,i},x_{v,i},v_{v,i},z_{f,i})$ is defined to be the right-hand side of Eq. 3, and $\hat{z}_f=[\hat{z}_{f,1}\ \dots\ \hat{z}_{f,m}]^T$. In addition, we define

$$z=\sum_{i=1}^{m} z_i \tag{6}$$

To clarify the valve model dynamics presented in this section, Figure 1 depicts a sliding-stem globe valve with a friction force and a force from the actuator acting upon it. This valve figure does not provide a detailed schematic of the inside of the valve, but helps to clarify how some of the forces described above may act on an example valve. It should also be noted that the discussion above is not limited to this sliding-stem globe valve type.

**Remark 1.** *We note that the form of Eqs. 2 and 3, which define the position and velocity of the valve using a force balance, implies that the moving parts of the valve under consideration move linearly, as would be the case with, for example, a sliding-stem globe valve. A variety of other valve types exist, however, and the moving parts of many of these do not move linearly, but rather rotate (this is the case with, e.g., a ball or butterfly valve).*[46–48] *Appropriate equations for the dynamics and friction for a valve that does not have linear movement could be substituted for Eqs. 2–5.*

**Remark 2.** *The data-driven friction models use decision-tree structures traversed based on the evaluation of Boolean expressions, and thus are not immediately in the first-order ordinary differential equation form of Eqs. 4 and 5. However, such models can be used to simulate a system and then perform a model identification procedure on the results to obtain a model in the form of Eqs. 4 and 5.*

*Relating valve position and valve output.* We relate $u_{a,i}$ to $x_{v,i}$ through the following nonlinear relationship

$$u_{a,i}=g_{V,i}(x_{v,i}) \tag{7}$$

where $g_{V,i}$ is a one-to-one continuous nonlinear function. We define $u_a=[u_{a,1}\ \dots\ u_{a,m}]^T$ and $g_V(x_v)=[g_{V,1}(x_{v,1})\ \dots\ g_{V,m}(x_{v,m})]^T$. As an example of possible relationships between $u_{a,i}$ and $x_{v,i}$, Figure 2 presents a plot of two types of relationships (linear and equal percentage) between $u_{a,i}$ and $x_{v,i}$ that are described in the literature for sliding-stem globe valves, and depicts the case that the zero of the valve position corresponds to zero flow.[28,46]

**Remark 3.** *As noted in* Ref. 28, *$u_{a,i}$ depends not only on $x_{v,i}$, but also on the fluid pressures upstream and downstream of the valve. In Eq. 7, we assume that the upstream and downstream pressures are fixed for a given value of $x_{v,i}$ such that we are able to write $u_{a,i}$ as a function of $x_{v,i}$ only by writing the pressure differential as a function of $x_{v,i}$ as well. However, for the case that this is not possible and the pressures are varying, it is possible to instead write Eq. 7 as a function of $x_{v,i}$ as well as of the upstream and downstream pressures and to still apply the method proposed in this article to the resulting system if the dynamics of the pressure variations are added to the process-valve model.*

*Linear controller dynamics.* It is customary in industry to implement a regulatory layer where classical linear controllers are used to influence the valve dynamics and force the valve output to be closer to the valve output set-point computed by the model predictive controller.[49] Thus, for consistency with industrial practice, we assume that a linear controller (e.g., a proportional (P) controller, a proportional-integral (PI), or a PID controller) is used, as opposed to a nonlinear controller, to regulate the valve stem position to its set-point. Because $x_{v,i}$ and $u_{a,i}$ are related through a one-to-one nonlinear algebraic equation, this is equivalent to assuming that the linear controller regulates the flow rate from the valve to its set-point. The dynamics of this linear controller are described by

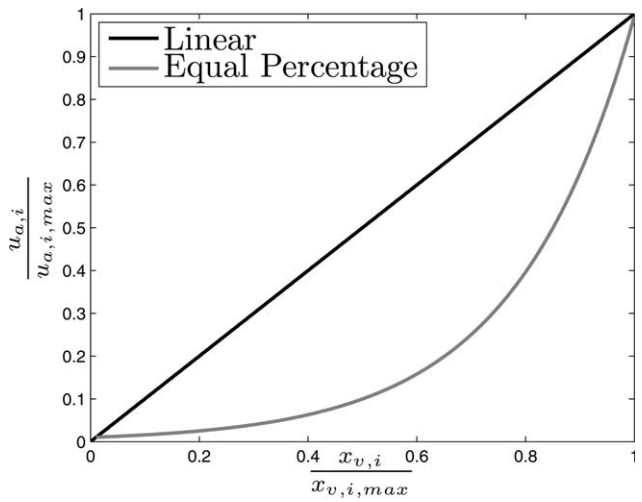


**Figure 2. Examples of relationships between $u_{a,i}$ and $x_{v,i}$ for a valve.**

**$x_{v,i,\max}$ is the maximum stem position of the valve. In this figure, $x_{v,i,\max}$ corresponds to the stem position when the valve is fully open.**

$$\dot{\zeta}_i = A_i \begin{bmatrix} x_{v,i} \\ \zeta_i \end{bmatrix} + B_i g_{V,i}^{-1}(u_{m,i}) \tag{8}$$

where $\zeta_i \in R^{r_i}$ is the vector of controller states for the linear controller of the $i$th valve output (this is the zero vector if a static controller is used), $u_{m,i}$ is the set-point for the valve output of the $i$th valve, which is set by the MPC, and $A_i \in R^{r_i \times (1+r_i)}$ and $B_i \in R^{r_i \times 1}$ are a matrix and a vector. In addition, we define $g_V^{-1}(u_m) = [g_{V,1}^{-1}(u_{m,1}) \ \dots \ g_{V,m}^{-1}(u_{m,m})]^T$ and

$$r = \sum_{i=1}^{m} r_i \tag{9}$$

*Combined process-valve model.* Given the differential and algebraic equations describing the dynamics of the process-valve system in Eqs. 1–9 to be controlled by MPC, we now combine these equations into one process-valve dynamic model with state vector $q = [x^T \ x_v^T \ v_v^T \ z_f^T \ \zeta^T]^T$

$$\dot{q} = \begin{bmatrix} \dot{x} \\ \dot{x}_v \\ \dot{v}_v \\ \dot{z}_f \\ \dot{\zeta} \end{bmatrix} = f_q(q(t), c(t), F_O(t), b(t), F_I(t), u_m(t), w(t))$$

$$= f_q(q(t), u_m(t), w(t)) = \begin{bmatrix} f(x(t), g_V(x_v(t)), w(t)) \\ v_v(t) \\ \hat{v}_v(c(t), F_O(t), b(t), F_I(t), x_v(t), v_v(t), z_f(t)) \\ \hat{z}_f(x_v(t), v_v(t), z_f(t)) \\ A \begin{bmatrix} x_v(t) \\ \zeta(t) \end{bmatrix} + B g_V^{-1}(u_m(t)) \end{bmatrix} \tag{10}$$

where $A$ and $B$ are matrices containing the entries of every $A_i$ and $B_i$, respectively, in appropriate orders. The statement that $f_q(q(t), c(t), F_O(t), b(t), F_I(t), u_m(t), w(t)) = f_q(q(t), u_m(t), w(t))$ follows because the vectors $c$, $F_O$, $b$, and $F_I$ will be functions of the states $q$ and/or the inputs $u_m$ when they are defined for a system.

Defining $q_v = n + 2m + z + r$, we assume that $f_q : R^{q_v} \times R^m \times R^w \to R^{q_v}$ is a locally Lipschitz function of its arguments with the origin of the unforced nominal system (the system of Eq. 10 with $u_m(t) \equiv 0$ and $w(t) \equiv 0$) at the origin (i.e., $f_q(0,0,0) = 0$). We further assume that the inputs $u_{m,i}$, $i = 1, \dots, m$, are restricted as follows: $u_{m,i} \in U_{m,i} := \{u_{m,i} \mid u_{m,i,\min} \le u_{m,i} \le u_{m,i,\max}\}$. It is noted that a valve set-point $u_{m,i}$ from the MPC need not be restricted to the same set $U_i$ that the actual valve output is restricted within (e.g., it may be restricted to a smaller set $U_{m,i}$ if it is known that the linear controller controlling the valve output overshoots the set-point). In addition to the restriction that each $u_{m,i} \in U_{m,i}$, we consider that there may be additional input constraints that depend on the current states, inputs, or both (as opposed to constraints that may depend on past and future values of the inputs or states). Thus, we consider that each $u_{m,i} \in U_{T,i}(q)$, where $U_{T,i}(q)$ represents the set of allowable values of the input $u_{m,i}$ given all constraints involving this input, and it is defined separately at each state-space point $q$ since the input constraints may depend on the current state.

We further assume that a Lyapunov-based controller $h_v(q) = [h_{v,1}(q) \ \dots \ h_{v,m}(q)]^T$ with $h_v(0) = 0$ exists for the nominal system of Eq. 10 that can render the origin locally asymptotically stable while meeting the input constraints in the sense that[50,51] a sufficiently smooth, positive definite Lyapunov function $V(q)$ and class $\mathcal{K}$ functions $\alpha_1(\cdot)$, $\alpha_2(\cdot)$, $\alpha_3(\cdot)$, and $\alpha_4(\cdot)$ exist that satisfy the following inequalities:

$$\alpha_1(|q|) \le V(q) \le \alpha_2(|q|) \tag{11a}$$

$$\frac{\partial V(q)}{\partial q} f_q(q, h_v(q), 0) \le -\alpha_3(|q|) \tag{11b}$$

$$\left| \frac{\partial V(q)}{\partial q} \right| \le \alpha_4(|q|) \tag{11c}$$

$$h_{v,i}(q) \in U_{T,i}(q), \ i = 1, \dots, m \tag{11d}$$

for all $q \in D \subseteq R^{q_v}$, where $D$ is an open neighborhood of the origin. A number of works address the development of Lyapunov-based control laws (see, e.g., Refs. 52–54).

There may be constraints on the states of the system of Eq. 10 (e.g., the constraint that each $u_{a,i} \in U_i$), which will restrict the allowable states within the set $Q$. The stability region of the process-valve system of Eq. 10 under the controller $h_v(q)$ is defined as the level set $\Omega_\rho \subseteq Q \subseteq D$ of the Lyapunov function. In addition to the requirements on $h_{v,i}$ in Eq. 11d, we require that each $h_{v,i}$, $i = 1, \dots, m$, be locally Lipschitz as follows

$$|h_{v,i}(q_1) - h_{v,i}(q_2)| \le L_v |q_1 - q_2|, \ i = 1, \dots, m \tag{12}$$

for all $q_1, q_2 \in \Omega_\rho$ where $L_v > 0$ can satisfy the Lipschitz condition for every $h_{v,i}$ (i.e., $L_v$ is greater than or equal to the minimum Lipschitz constant that can satisfy the Lipschitz condition for the control law $h_{v,i}$ that has the largest minimum Lipschitz constant from all $i = 1, \dots, m$). We note that when $h_v(q)$ is applied to the system of Eq. 10 in sample-and-hold, it can render the origin practically stable for sampling periods $\Delta \le \Delta^*$.[55]

From Lipschitz continuity of $f_q$, from the bounds on $u_{m,i}$ and $w$, and from the fact that $V(q)$ is sufficiently smooth, there exist positive constants $M$, $L_q$, $L_w$, $L'_q$, and $L'_w$ such that

$$|f_q(q, u_{m,1}, \dots, u_{m,m}, w)| \le M \tag{13}$$

$$|f_q(q_1, u_{m,1}, \dots, u_{m,m}, w) - f_q(q_2, u_{m,1}, \dots, u_{m,m}, 0)| \le L_q |q_1 - q_2| + L_w |w| \tag{14}$$

$$\left| \frac{\partial V(q_1)}{\partial q} f_q(q_1, u_{m,1}, \dots, u_{m,m}, w) - \frac{\partial V(q_2)}{\partial q} f_q(q_2, u_{m,1}, \dots, u_{m,m}, 0) \right| \le L'_q |q_1 - q_2| + L'_w |w| \tag{15}$$

for all $q, q_1, q_2 \in \Omega_\rho$, $u_{m,i} \in U_{T,i}(q)$, $i = 1, \dots, m$, and $|w| \le \theta$. A consequence of Eq. 13 and the continuity of $q$ is that the following inequality holds

$$|q(t)-q(t_{k-1})| \leq M\Delta \tag{16}$$

for all $q(t), q(t_{k-1}) \in \Omega_\rho$ when $t \in [t_{k-1}, t_k]$, and a $\Delta$ sufficiently small (i.e., $\Delta < \Delta_1$, where $\Delta_1$ is the largest value of $\Delta$ for which Eq. 16 holds).

**Remark 4.** *In Eq. 10, disturbance is only considered in the process states. It is noted that disturbance could also be added to the states $x_v$, $v_v$, and $z_f$ if desired, and all results in this article would continue to hold if the resulting noise vector was bounded as w is assumed to be.*

### *Model predictive control*

MPC is a control strategy characterized by the use of an optimization problem incorporating a process model to compute control actions throughout a prediction horizon subject to process constraints. Tracking MPC, generally formulated with a quadratic objective and designed to regulate a process to a steady-state, is popular in the chemical processing industry,[56] but other formulations of MPC, such as economic model predictive control,[57–59] incorporate a nonlinear objective function that does not have its minimum at a steady-state. In this work, we develop a stiction compensation methodology using stiction dynamics incorporated in the MPC process model, and the strategy developed is suitable for any MPC formulation. A general formulation of MPC has the form

$$\min_{u_{m,1}(t),\ldots,u_{m,m}(t)\in S(\Delta)} \int_{t_k}^{t_{k+N}} L_{\text{MPC}}(\tilde{x}(\tau), u_{m,1}(\tau), \ldots, u_{m,m}(\tau))\, d\tau \tag{17a}$$

$$\text{s.t. } \dot{\tilde{x}}(t) = f(\tilde{x}(t), u_{m,1}(t), \ldots, u_{m,m}(t), 0) \tag{17b}$$

$$\tilde{x}(t_k) = x(t_k) \tag{17c}$$

$$\tilde{x}(t) \in X,\ \forall\, t \in [t_k, t_{k+N}) \tag{17d}$$

$$u_{m,i}(t) \in U_{m,i},\ i=1,\ldots,m,\ \forall\, t \in [t_k, t_{k+N}) \tag{17e}$$

$$g_{\text{MPC},1}(\tilde{x}(t), u_{m,1}(t), \ldots, u_{m,m}(t)) = 0 \tag{17f}$$

$$g_{\text{MPC},2}(\tilde{x}(t), u_{m,1}(t), \ldots, u_{m,m}(t)) \leq 0 \tag{17g}$$

where the optimal control trajectories are chosen among all functions in the set $S(\Delta)$ of piecewise-constant functions with period $\Delta$. A general stage cost $L_{\text{MPC}}(x(t), u_{m,1}(t), \ldots, u_{m,m}(t))$ is optimized (Eq. 17a) subject to constraints on the predicted state $\tilde{x}(t)$ that limit it to the state-space region $X$ (Eq. 17d), bounds on the allowable control actions (Eq. 17e), and general equality (Eq. 17f) and inequality (Eq. 17g) constraints described by functions $g_{\text{MPC},1}(x(t), u_{m,1}(t), \ldots, u_{m,m}(t))$ and $g_{\text{MPC},2}(x(t), u_{m,1}(t), \ldots, u_{m,m}(t))$, respectively. Predictions of the process state are obtained from the differential equation for the process in Eq. 17b and the initial condition in Eq. 17c obtained from a state measurement of the process at time $t_k$. MPC is implemented in a receding horizon fashion by solving the MPC optimization problem in Eq. 17 to determine $N$ vectors $u_m$ of sample-and-hold input trajectories corresponding to the $N$ sampling periods in the prediction horizon. Only the vector of control actions corresponding to the first sampling period of the prediction horizon is implemented on the process, and at the next sampling time, the MPC is resolved.

## MPC for Stiction Compensation

A stiction compensation strategy should address the negative effects of stiction on control loop performance, including that it can prevent a valve from effectively tracking the setpoints it receives or can result in oscillations in a control loop. Another negative effect of stiction can be changes in the valve dynamics as stiction worsens that affect the range of values that the valve output can take with the available actuation energy. The proposed MPC can alleviate these negative impacts of valve stiction. We first discuss the proposed control loop architecture, and then proceed to develop the model predictive controller formulation incorporating the process and valve dynamics, actuation magnitude constraints, and input rate of change constraints. We also include Lyapunov-based stability constraints that will be used to prove feasibility of the proposed MPC optimization problem and stability of the closed-loop system under the MPC. We discuss how the proposed formulation addresses the various issues associated with stiction and provide the proofs of feasibility and closed-loop stability for a sufficiently small sampling period.

### *MPC architecture and formulation for stiction compensation*

The proposed control architecture, shown in Figure 3, incorporates an MPC controlling a process by providing set-points for the valve outputs (process manipulated inputs) to a linear controller that drives the valve output quickly to its set-point. It is noted that the control of the valve output set-point, rather than the stem position itself, is a feature of the methodology and is chosen for consistency with the current control architectures incorporating MPC and a lower layer with linear controllers in industry. The proposed MPC computes control actions by solving the following optimization problem

$$\min_{u_{m,1}(t),\ldots,u_{m,m}(t)\in S(\Delta)} \int_{t_k}^{t_{k+N}} L_{\text{MPC}}(\tilde{q}(\tau), u_{m,1}(\tau), \ldots, u_{m,m}(\tau))\, d\tau \tag{18a}$$

$$\text{s.t. } \dot{\tilde{q}}(t) = f_q(\tilde{q}(t), u_{m,1}(t), \ldots, u_{m,m}(t), 0) \tag{18b}$$

$$\tilde{q}(t_k) = q(t_k) \tag{18c}$$

$$\tilde{q}(t) \in Q,\ \forall\, t \in [t_k, t_{k+N}) \tag{18d}$$

$$u_{m,i}(t) \in U_{m,i},\ \forall\, i=1,\ldots,m,\ t \in [t_k, t_{k+N}) \tag{18e}$$

$$g_{\text{act},1}(\tilde{q}(t), u_{m,1}(t), \ldots, u_{m,m}(t)) = 0,\ \forall\, t \in [t_k, t_{k+N}) \tag{18f}$$

$$g_{\text{act},2}(\tilde{q}(t), u_{m,1}(t), \ldots, u_{m,m}(t)) \leq 0,\ \forall\, t \in [t_k, t_{k+N}) \tag{18g}$$

$$|u_{m,i}(t_k) - h_{v,i}(q(t_k))| \leq \epsilon,\ i=1,\ldots,m \tag{18h}$$

$$|u_{m,i}(t_j) - h_{v,i}(\tilde{q}(t_j))| \leq \epsilon,\ i=1,\ldots,m,\ j=k+1,\ldots,k+N-1 \tag{18i}$$

$$g_{\text{MPC},1}(\tilde{q}(t), u_{m,1}(t), \ldots, u_{m,m}(t)) = 0,\ \forall\, t \in [t_k, t_{k+N}) \tag{18j}$$

$$g_{\text{MPC},2}(\tilde{q}(t), u_{m,1}(t), \ldots, u_{m,m}(t)) \leq 0,\ \forall\, t \in [t_k, t_{k+N}) \tag{18k}$$

$$V(\tilde{q}(t)) \leq \rho_e,\ \forall\, t \in [t_k, t_{k+N}) \text{ if } t_k < t' \text{ and } V(q(t_k)) \leq \rho_e \tag{18l}$$

$$\frac{\partial V(q(t_k))}{\partial q} f_q(q(t_k), u_{m,1}(t_k), \ldots, u_{m,m}(t_k), 0) \leq \frac{\partial V(q(t_k))}{\partial q} f_q(q(t_k), h_{v,1}(q(t_k)), \ldots, h_{v,m}(q(t_k)), 0) \text{ if } t_k \geq t' \text{ or } V(q(t_k)) > \rho_e \tag{18m}$$

This MPC is implemented in the same manner as Eq. 17; however, here the general stage cost $L_{\text{MPC}}$ (Eq. 18a) is a function of the predicted state $\tilde{q}$ from the full process-valve model

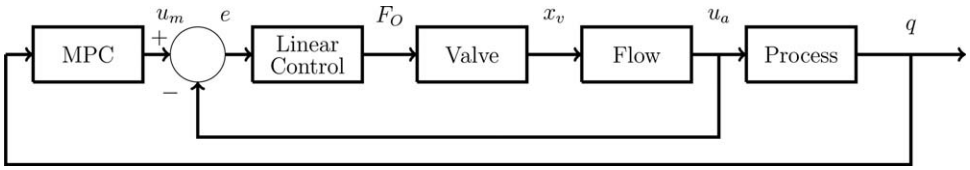


**Figure 3. Proposed architecture for MPC incorporating valve dynamics and actuation magnitude constraints for stiction compensation.**

**For simplicity of presentation, the only force on the valve presented is one which is calculated by the linear controller.**

(Eq. 18b, with initial condition in Eq. 18c) and the vector of valve set-points $u_m$, which is the decision variable of the optimization problem. The solution to the optimization problem of Eq. 18 at time $t_k$ is denoted by $u^*_{m,i}(t|t_k)$, $i=1, \ldots, m$, $t=t_k, t_{k+1}, \ldots, t_{k+N-1}$. In Eq. 18, the predicted state $\tilde{q}$ is restricted to the set $Q$ (Eq. 18d), and each manipulated input $u_{m,i}$ is restricted to the set $U_{m,i}$, $i=1, \ldots, m$ (Eq. 18e) (note that the predicted values of $u_{a,i}$ are restricted by Eqs. 18d and 7). In addition to such constraints on the actuation of each valve, the use of the detailed stiction model within the MPC allows additional restrictions to be placed on the actuation magnitude, including the equality and inequality constraints in Eqs. 18f and 18g, to prevent the MPC from calculating undesirable or nonphysical set-points $u_{m,i}$ (these constraints were written with the states and inputs as arguments, although they are functions of $b(t)$, $F_O(t)$, $c(t)$, and $F_I(t)$, using the simplification noted in Section "Combined Process-Valve Model" that $b(t)$, $F_O(t)$, $c(t)$, and $F_I(t)$ will be functions of the states and inputs when they are explicitly defined for the given valve). Input rate of change constraints can also be added, as in Eqs. 18h and 18i. The input rate of change constraints are written with respect to the controller $h_{v,i}$, but it can be proven (see Proposition 3 below) that for a given $\epsilon_{\text{desired}}$ the constraints, when written in this manner, constrain the rates of change $|u_{m,i}(t_k) - u^*_{m,i}(t_{k-1}|t_{k-1})| \leq \epsilon_{\text{desired}}$ and $|u_{m,i}(t_j) - u_{m,i}(t_{j-1})| \leq \epsilon_{\text{desired}}$, $j=k+1, \ldots, k+N-1$, when a sufficiently small sampling period $\Delta$ and an appropriate value of $\epsilon$ are chosen. Eqs. 18j and 18k are general nonlinear equality and inequality constraints that can be added to the optimization problem to achieve desired performance goals. As stated in Section "Combined Process-Valve Model," we require that the constraints in Eqs. 18f, 18g and 18j, 18k be constraints defined point-wise in space (they only depend on the current states and inputs, and not on past values of these variables).

In addition to the constraints designed to improve process performance in the presence of stiction, the Lyapunov-based constraints in Eqs. 18l and 18m have been added to prove feasibility and closed-loop stability of the proposed MPC formulation. These constraints define two modes of operation of the MPC. When the constraint of Eq. 18l is active, Mode 1 of the MPC is active and the process performance is optimized to the maximum extent possible within a subset of the stability region, $\Omega_{\rho_e} \subset \Omega_\rho$, which is defined such that if the MPC is initialized at time $t_k$ from any state within $\Omega_{\rho_e}$, the state at time $t_{k+1}$ is still within $\Omega_\rho$. This Mode 1 constraint is specific to Lyapunov-based economic model predictive control,[57] the goal of which is to maximize the process profit to the maximum extent possible using dynamic operation in Mode 1. In Mode 2, the contractive constraint in Eq. 18m drives the state to a neighborhood of the origin. Mode 1 and Mode 2 are activated by either the location of the measured state in state-space, or by the current time ($t\prime$ denotes the time at which process operation switches from Mode 1 to Mode 2). For tracking MPC, the Mode 2 constraint would be active for all times (i.e., $t\prime=0$ and the MPC formulation in Eq. 18 is like that proposed as Lyapunov-based model predictive control in Ref. 60).

**Remark 5.** *Due to the generality of the proposed MPC formulation, it is possible for a different stabilizing formulation, such as a terminal cost with a terminal region constraint,*[61,62] *a terminal state constraint,*[63,64] *or an infinite horizon,*[65] *to be used in place of Eqs. 18l and 18m (see also* Refs. 66 and 67 *and the references therein for more information on various types of constraints that can be used in MPC and EMPC). However, due to the ease of establishing the state-space points from which feasibility and closed-loop stability are guaranteed using Eqs. 18l and 18m and the fact that these properties can be proven for the process under the MPC with those constraints without any assumptions on the cost function structure, we choose to establish feasibility and stability of the proposed method in this work using the stability constraints in Eqs. 18l and 18m.*

**Remark 6.** *In a practical setting, the parameters of the stiction model may change with time as stiction worsens. Thus, it may be desirable to reidentify the parameters of the stiction model at various points in time. In addition, it may be necessary to retune the linear controller of the valve as its dynamics change due to stiction. Thus, an assumption of the proposed design is that one can successfully detect and identify stiction and retune the controller as desired. Although stiction detection and quantification are outside the scope of this work, a number of results have appeared in these research fields, including methods based on trends in controller output and controlled variable data (e.g.,* Refs. 68 and 69*) or those based on model identification (e.g.,* Refs. 2, 7, and 12*); see also the review paper* Ref. 8 *and the references therein. With regard to the retuning of the linear controller, controller tuning methods are discussed in works such as* Refs. 70–72.

**Remark 7.** *As commonly noted in the literature, the negative impact of valve stiction cannot be fully remedied unless valve maintenance is performed.*[36] *However, there are circumstances in which maintenance is not performed on sticky valves until a planned process shutdown, which is often infrequent (every 6 months to 3 years).*[33] *The growing body of developments in stiction assessment and the use of MPC to prevent process shut-down during actuator maintenance make the proposed stiction compensation architecture ideal for integration with these other developments to allow one to detect growing valve stiction but then to perform the maintenance without waiting for a process shut-down. As suggested in the literature (e.g.,* Refs. 34 and 35*), methods for online stiction detection and quantification*[29,73,74] *could be used by a scheduler or decision-maker to develop a valve maintenance schedule. Actuator preventive maintenance strategies that use MPC to allow for the maintenance of a valve while maintaining process operation and closed-loop stability can then be applied.*[75]

### *Analysis of MPC formulation*

The power of the proposed stiction compensation strategy lies in its flexibility. Because of the incorporation of the stiction dynamics in the MPC, a control engineer can adjust the cost function and the constraints to minimize the negative impacts of stiction, including the delay in a valve's response to a control signal change, control loop oscillations, and changes in the relationship between the valve output and actuation magnitude as stiction worsens. To clarify this point, we present a number of remarks that exemplify how the proposed MPC could be modified to counter various control loop issues due to stiction.

**Remark 8.** *The linear controller for the valve can be used to speed the response of the valve to a set-point change, even a set-point change in the direction opposite to previous set-point changes (i.e., a set-point change that causes the valve to stick). If the controller is aggressive, it can cause the control input to the valve to quickly overcome the deadband, reducing set-point tracking issues arising from stiction (if the aggressiveness does not cause oscillations).*

**Remark 9.** *The MPC cost function could include a penalty on deviations of the valve output from its set-point throughout time. Because the MPC incorporates a model of the stiction dynamics and thus is aware that the valve will slip and by how much, this penalty would encourage the MPC to choose, as often as possible, set-points that are not within the range of valve outputs where slip-jump occurs, or which are at values at which the valve output can be stabilized even if the integral term of the linear controller becomes large during the direction change of the valve velocity.*

**Remark 10.** *If stiction is affecting a valve significantly such that the control loop is oscillating and the proposed method is implemented with an economics-based objective, the proposed method could be used to choose set-points that are more economically optimal than if the MPC was unaware of the process dynamics. For example, even if a set-point was chosen about which the valve output (and consequently the process variables controlled by this valve output) oscillated, this would still be the most economically optimal method for operating the system because the MPC included the oscillatory effect of the valve dynamics in its determination of the optimal valve set-points.*

**Remark 11.** *If the linear controller is appropriately designed, the input rate of change constraints in Eqs. 18h and 18i can be added to prevent the integral term of the linear controller from growing large for any given set-point change, reducing the likelihood that there will be a wind-up-like effect caused by the deadband/stickband of the valve. For example, if the linear controller is designed such that its output is the force that the valve actuator must apply to the valve, the integral term of the linear controller could be reset to 0 at the beginning of each sampling period, and the steady-state value of the linear controller output could be set to the last applied value of the controller output. Thus, the force on the valve from the valve actuator could be increased gradually throughout a number of sampling periods where small changes of the valve set-point occur in each, such that it is less likely that the integral term will be large when the linear controller output becomes large enough to initiate slip-jump of the valve. This is consistent with the concept used in stiction compensation strategies such as the knocker and constant reinforcement of adding compensating pulses to the control signal in an attempt to make the valve slip with a lower value of the integral action than if compensation were not used.*[26,29]

**Remark 12.** *A major contribution of the proposed method is that it accounts for changes in the range of valve outputs that can be achieved with the given actuation energy as stiction worsens. This has not been addressed by prior stiction compensation methods. It is less of a concern for stiction compensation methods that only adjust the control signal to the valve (rather than the valve set-point) because the valve actuation magnitude can saturate if the control signal exceeds its limits, and when the set-point remains constant, it is less likely that the extremes of the valve actuation magnitude will be approached. The previous MPC strategies for stiction compensation have also not explicitly addressed the change in constraints that results as the valve output-actuation magnitude dynamics change, although* Refs. 42–44 *address valve output saturation. The proposed method of this work, however, introduces actuation magnitude constraints in Eqs. 18f and 18g to constrain the valve actuation magnitude and prevent the process-valve model from predicting nonphysical values for such forces. This will be further clarified in Section "Application to a Chemical Process Example" in this work.*

**Remark 13.** *Some stiction compensation methods such as constant reinforcement and the knocker that add signals to the output of the controller being sent to the valve are cited as sources of valve wear and tear, which makes these methods short-term solutions.*[29,31] *Several stiction compensation strategies have been developed to address this, including an optimization-based stiction compensation method that minimizes a cost function including a term representing the degree of movement of the valve to seek compensating signals to add to the valve controller output that will minimize the valve movement.*[33] *The MPC stiction compensation method proposed in this article is flexible and could include similar penalties in the objective if valve wear and tear is a concern.*

### *Feasibility and stability*

In this section, we prove that the optimization problem of Eq. 18 is feasible for all times and that the closed-loop system of Eq. 10 is stable under the MPC of Eq. 18 when a sufficiently small sampling period is used. We first restate two propositions from Ref. 57 used to define parameters and equations that will be used in the feasibility and stability proof. We then motivate the introduction of a constraint that we will impose on $\Delta$ in the proof by a proposition that shows that the input rate of change constraints as formulated with respect to the Lyapunov-based controller $h_v(q)$ in Eqs. 18h and 18i constrain the difference between consecutively applied solutions of the MPC optimization problem to be less than a desired value (these input rate of change constraints for MPC are different than those in previous works on input rate of change constraints in MPC such as, e.g., Ref. 76). Finally, we combine the results of the propositions to prove feasibility and stability of the proposed MPC.

**Proposition 1**. *(c.f.* Refs. 57 and 77*). Consider the systems*

$$\dot{q}_a(t) = f_q(q_a(t), u_{m,1}(t), \ldots, u_{m,m}(t), w(t)) \tag{19a}$$

$$\dot{q}_b(t) = f_q(q_b(t), u_{m,1}(t), \ldots, u_{m,m}(t), 0) \tag{19b}$$

*with initial states $q_a(t_0) = q_b(t_0) \in \Omega_\rho$. There exists a $\mathcal{K}$ function $f_W(\cdot)$ such that*

$$|q_a(t) - q_b(t)| \leq f_W(t - t_0) \tag{20}$$

*for all $q_a(t), q_b(t) \in \Omega_\rho$ and all $w(t) \in W$ with*

$$f_W(\tau)=\frac{L_w\theta}{L_q}(e^{L_q\tau}-1) \tag{21}$$

**Proposition 2**. *(c.f.* Refs. 57 and 77*). Consider the Lyapunov function $V(\cdot)$ of the nominal system of Eq. 10 under the controller $h_v(q)$. There exists a quadratic function $f_V(\cdot)$ such that*

$$V(q) \le V(\hat{q})+f_V(|q-\hat{q}|) \tag{22}$$

*for all $q, \hat{q} \in \Omega_\rho$ with*

$$f_V(s)=\alpha_4(\alpha_1^{-1}(\rho))s+M_v s^2 \tag{23}$$

*where $M_v$ is a positive constant.*

**Proposition 3**. *Consider the system of Eq. 10 in closed-loop with the MPC of Eq. 18. If a Lyapunov-based controller $h_v(q)$ that meets the assumptions of Eqs. 11 and 12 exists, then the constraints of Eqs. 18h and 18i ensure that for a given $\epsilon_{\text{desired}}$*

$$|u_{m,i}(t_k)-u^*_{m,i}(t_{k-1}|t_{k-1})| \le \epsilon_{\text{desired}} \tag{24}$$

*and*

$$|u_{m,i}(t_j)-u_{m,i}(t_{j-1})| \le \epsilon_{\text{desired}},\ j=k+1,\ldots,k+N-1 \tag{25}$$

*when $\Delta \le \min(\Delta_1, \Delta^*)$ and $\epsilon$ in Eqs.* 18h *and* 18i *are chosen such that*

$$2\epsilon+L_vM\Delta \le \epsilon_{\text{desired}} \tag{26}$$

**Proof.** From the bound in Eq. 16 and the Lipschitz continuity of $h_{v,i}(q)$ in Eq. 12, for every $\epsilon_{\text{continuous}}>0$, there exists $\delta(\epsilon_{\text{continuous}})>0$ such that if

$$|q(t_k)-q(t_{k-1})| \le M\Delta < \delta \tag{27}$$

and

$$|\tilde{q}(t_j)-\tilde{q}(t_{j-1})| \le M\Delta < \delta \tag{28}$$

for all $j=k+1,\ldots,k+N-1$, then

$$|h_{v,i}(q(t_k))-h_{v,i}(q(t_{k-1}))| \le L_v|q(t_k)-q(t_{k-1})| \le L_vM\Delta < \epsilon_{\text{continuous}} \tag{29}$$

and

$$|h_{v,i}(\tilde{q}(t_j))-h_{v,i}(\tilde{q}(t_{j-1}))| \le L_v|\tilde{q}(t_j)-\tilde{q}(t_{j-1})| \le L_vM\Delta < \epsilon_{\text{continuous}} \tag{30}$$

for a sufficiently small $\Delta \le \min(\Delta_1, \Delta^*)$ and $q(t_k), \tilde{q}(t_j), \tilde{q}(t_{j-1}) \in \Omega_\rho$ for $j=k+1,\ldots,k+N-1$. Combining this with Eqs. 18h and 18i, it is shown that

$$\begin{aligned}|u_{m,i}(t_k) - u^*_{m,i}(t_{k-1}|t_{k-1})| &= |u_{m,i}(t_k) - u^*_{m,i}(t_{k-1}|t_{k-1}) \\ &- h_{v,i}(q(t_k)) + h_{v,i}(q(t_k)) - h_{v,i}(q(t_{k-1})) \\ &+ h_{v,i}(q(t_{k-1}))| \le |u_{m,i}(t_k) - h_{v,i}(q(t_k))| + |u^*_{m,i}(t_{k-1}|t_{k-1}) \\ &- h_{v,i}(q(t_{k-1}))| + |h_{v,i}(q(t_k)) - h_{v,i}(q(t_{k-1}))| \le 2\epsilon + L_vM\Delta\end{aligned}$$

and

$$\begin{aligned}|u_{m,i}(t_j) - u_{m,i}(t_{j-1})| &= |u_{m,i}(t_j) - u_{m,i}(t_{j-1}) - h_{v,i}(\tilde{q}(t_j)) \\ &+ h_{v,i}(\tilde{q}(t_j)) - h_{v,i}(\tilde{q}(t_{j-1})) + h_{v,i}(\tilde{q}(t_{j-1}))| \le |u_{m,i}(t_j) \\ &- h_{v,i}(\tilde{q}(t_j))| + |u_{m,i}(t_{j-1}) - h_{v,i}(\tilde{q}(t_{j-1}))| + |h_{v,i}(\tilde{q}(t_j)) \\ &- h_{v,i}(\tilde{q}(t_{j-1}))| \le 2\epsilon + L_vM\Delta\end{aligned}$$

for $j=k+1,\ldots,k+N-1$. Thus, the desired constraints in Eqs. 24 and 25 are satisfied when $2\epsilon+L_vM\Delta \le \epsilon_{\text{desired}}$. ■

**Theorem 1.** *Consider the system of Eq. 10 in closed-loop under the MPC design of Eq. 18 based on a controller $h_v(q)$ that satisfies the conditions of Eqs. 11 and 12 and assume that $u_i^*(t_0|t_0)=h_i(x(t_0))$, $i=1,\ldots,m$. Let $\epsilon_w>0$, $0<\Delta \le \min(\Delta_1, \Delta^*)$, $\theta>0$, $\rho>\rho_e\ge\rho_s>0$ satisfy*

$$\rho_e \le \rho - f_V(f_W(\Delta)) \tag{31}$$

$$-\alpha_3(\alpha_2^{-1}(\rho_s))+L'_qM\Delta+L'_w\theta \le \frac{-\epsilon_w}{\Delta} \tag{32}$$

*and*

$$2\epsilon+L_vM\Delta \le \epsilon_{\text{desired}} \tag{33}$$

*If $q(t_0)\in\Omega_\rho$, $\rho_s \le \rho_{\min}$, and $N\ge 1$ where*

$$\rho_{\min}=\max\{V(q(t+\Delta)) : V(q(t)) \le \rho_s\} \tag{34}$$

*then the state $q(t)$ of the closed-loop system is always bounded in $\Omega_\rho$ and is ultimately bounded in $\Omega_{\rho_{\min}}$.*

**Proof.** Feasibility of the proposed formulation will be proven by showing that when the Lyapunov-based controller $h_v(q)$ exists that satisfies the constraints in Eqs. 11 and 12, it is a feasible solution for the MPC optimization problem at all times if $q(t)\in\Omega_\rho$ for all times. The proof of the closed-loop stability of the proposed method follows that in Ref. 57 and will not be repeated here, but it shows that the proposed MPC of Eq. 18 can maintain the states within the region $\Omega_\rho$ for all times if a small enough sampling period is used. Closed-loop stability of a process under the proposed MPC follows from Ref. 57 with the only bounds on $\Delta$ being those in Eqs. 31 and 32. In this theorem, to obtain the desired rates of change in Eqs. 24 and 25, we also add the requirement from Proposition 3 that Eq. 33 must be satisfied as well; however, this is not required for closed-loop stability to be proven.

The feasibility of the state, input, Lyapunov-based, and input rate of change constraints will be addressed when $u_{m,i}(t_k)=h_{v,i}(q(t_k))$ and $u_{m,i}(t_j)=h_{v,i}(\tilde{q}(t_j))$, $j=k+1,\ldots,k+N-1$, and $q(t_k), \tilde{q}(t)\in\Omega_\rho$. Due to the definition of the stability region $\Omega_\rho$, which included the requirement that it be a region within which all state constraints are satisfied, the state constraint in Eq. 18d is satisfied for all states within $\Omega_\rho$. Also, by Eq. 11d, $h_{v,i}(q(t_k))$ and $h_{v,i}(\tilde{q}(t_j))$, $j=k+1,\ldots,k+N-1$, satisfy the input constraints in Eqs. 18e–18g and 18j, 18k. Furthermore, by design of the Lyapunov-based constraints and when $\Delta\le\Delta^*$, $h_{v,i}(q(t_k))$ and $h_{v,i}(\tilde{q}(t_j))$, $j=k+1,\ldots,k+N-1$, satisfy the Lyapunov-based constraints in Eqs. 18l and 18m. Finally, by design of the input rate of change constraints in Eqs. 18h and 18i with respect to the Lyapunov-based control law, $h_{v,i}(q(t_k))$ and $h_{v,i}(\tilde{q}(t_j))$, $j=k+1,\ldots,k+N-1$, also satisfy those equations. Thus, feasibility of the proposed MPC at each sampling time is ensured. ■

## Application to a Chemical Process Example

In this section, we present a case study that shows how an MPC incorporating stiction dynamics may be designed for a specific chemical process example. For this study, we focus on EMPC because EMPC can dictate a dynamic operating policy, which has interesting implications for the constraints that need to be added to the EMPC for effective stiction compensation in this example, and thus helps to illustrate the considerations that may go into the design of the MPC in Eq. 18 to ensure that it adequately prevents the negative effects of stiction.

### *Dynamic model development*

We first define the detailed valve and process models that will be used in this example.

*Nonlinear Process Model.* We consider control of the catalytic oxidation of ethylene in a continuously stirred tank reactor for which the following reactions occur

$$C_2H_4 + \frac{1}{2}O_2 \rightarrow C_2H_4O \tag{35a}$$

$$C_2H_4 + 3O_2 \rightarrow 2CO_2 + 2H_2O \tag{35b}$$

$$C_2H_4O + \frac{5}{2}O_2 \rightarrow 2CO_2 + 2H_2O \tag{35c}$$

The dimensionless material and energy balances for this process from Ref. 78, which use reaction rate equations from Ref. 79, form the following nonlinear process model of the system

$$\frac{dx_1}{dt} = u_a(1 - x_1x_4) \tag{36a}$$

$$\frac{dx_2}{dt} = u_a(C_e - x_2x_4) - A_1\exp\left(\frac{\gamma_1}{x_4}\right)(x_2x_4)^{0.5} - A_2\exp\left(\frac{\gamma_2}{x_4}\right)(x_2x_4)^{0.25} \tag{36b}$$

$$\frac{dx_3}{dt} = -u_ax_3x_4 + A_1\exp\left(\frac{\gamma_1}{x_4}\right)(x_2x_4)^{0.5} - A_3\exp\left(\frac{\gamma_3}{x_4}\right)(x_3x_4)^{0.5} \tag{36c}$$

$$\begin{aligned}\frac{dx_4}{dt} = \frac{1}{x_1}\Big(&u_a(1 - x_4) + B_1\exp\left(\frac{\gamma_1}{x_4}\right)(x_2x_4)^{0.5} \\ &+ B_2\exp\left(\frac{\gamma_2}{x_4}\right)(x_2x_4)^{0.25} + B_3\exp\left(\frac{\gamma_3}{x_4}\right)(x_3x_4)^{0.5} \\ &- B_4(x_4 - T_c)\Big)\end{aligned} \tag{36d}$$

where $x_1$, $x_2$, $x_3$, and $x_4$ are the dimensionless quantities corresponding to the gas density in the reactor, the reactor ethylene and ethylene oxide concentrations, and the reactor temperature, respectively. The process input (valve output) $u_a$ is the dimensionless volumetric flow rate of the feed. The dimensionless concentration of ethylene in the feed ($C_e$) and the dimensionless coolant temperature $T_c$ are set to their values corresponding to an open-loop asymptotically stable steady-state of the reactor (the asymptotically stable steady-state occurs at $[x_{1s}\,x_{2s}\,x_{3s}\,x_{4s}] = [0.998\ 0.424\ 0.032\ 1.002]$ when $u_{as} = 0.35$, $C_e = 0.5$, and $T_c = 1.0$). The other parameters in Eq. 36 are taken from Ref. 78 and are noted in Table 1.

*Nonlinear Valve Model.* In this section, we describe the model of the valve dynamics for the valve that adjusts $u_a$. Due to their prevalence in industry, we model a pneumatic spring-diaphragm sliding-stem globe valve using the values for the valve parameters from Ref. 4, with the exception that the time units of all parameters are changed to the dimensionless time unit $t_d$ for consistency with the time units in the process model of Eq. 36, and are given in Table 1. The valve is modeled as a pressure-to-close valve with no pressure applied by the pneumatic actuation at the fully open valve position. The valve stem can travel a maximum of 0.1016 m from the fully open valve position (which corresponds to the flow rate $u_a = 0.7042$) to the fully closed position (with corresponding flow rate $u_a = 0$). Figures 4 and 5 depict the fully open and fully closed valve positions; however, these are not detailed drawings of the valve interior and are meant only for clarification of how the stem's location is related to the valve opening. In accordance with Refs. 3–5, we assume that the following differential equations are sufficient for describing the stem position and velocity for the valve adjusting $u_a$ (i.e., as in Refs. 3–5, we neglect additional forces known to be present in sliding-stem globe valves, such as the additional force required to move the valve plug into the seat and the force due to the pressure drop of the fluid as it moves through the valve)

$$\frac{dx_v}{dt} = v_v \tag{37}$$

$$\frac{dv_v}{dt} = \frac{1}{m_v}[A_vP - kx_v - F_f] \tag{38}$$

where the notation follows that in Eqs. 2 and 3, with $A_v$ being the area of the valve diaphragm to which the actuator applies a pressure $P$ determined from the linear controller for the valve, and $k$ is the spring constant of the spring that opposes the movement of the diaphragm when pressure is applied. We associate the fully open position of the valve with the equilibrium spring position $x_v = 0$ m, and we associate the fully closed valve position with the maximum stem position $x_v = x_{v,\max} = 0.1016$ m.

To determine the value of $F_f$ in Eq. 38 at each time instant, we use the LuGre[16] friction model due to its relative simplicity (it is a dynamic model with only one differential equation) and ability to qualitatively describe many of the effects of friction (e.g., presliding displacement, hysteresis in the friction force with velocity changes in the sliding regime, and a lowering of the force required for breakaway as the applied force increases more quickly[16]; also see Ref. 4 for information on the ability of a valve simulated using the LuGre model and the valve parameters in this article to qualitatively exhibit the behavior expected when subjected to valve tests developed by the Instrumentation, Systems, and Automation Society). The LuGre model describes friction using the following differential and algebraic equations[16]

**Table 1. Process and Valve Parameters[4,78]**

| Parameter | Value | Parameter | Value |
|---|---|---|---|
| $\gamma_1$ | −8.13 | $m_v$ | 1.361 kg |
| $\gamma_2$ | −7.12 | $A_v$ | 0.06452 $m^2$ |
| $\gamma_3$ | −11.07 | $k$ | 52,538 $kg/t_d^2$ |
| $A_1$ | 92.80 | $\sigma_0$ | $10^8$ $kg/t_d^2$ |
| $A_2$ | 12.66 | $v_s$ | 0.000254 $m/t_d$ |
| $A_3$ | 2412.71 | $\sigma_1$ | 9000 $kg/t_d$ |
| $B_1$ | 7.32 | $\sigma_2$ | 612.9 $kg/t_d$ |
| $B_2$ | 10.39 | $F_C$ | 1423 $kg{\cdot}m/t_d^2$ |
| $B_3$ | 2170.57 | $F_S$ | 1707.7 $kg{\cdot}m/t_d^2$ |
| $B_4$ | 7.02 | | |

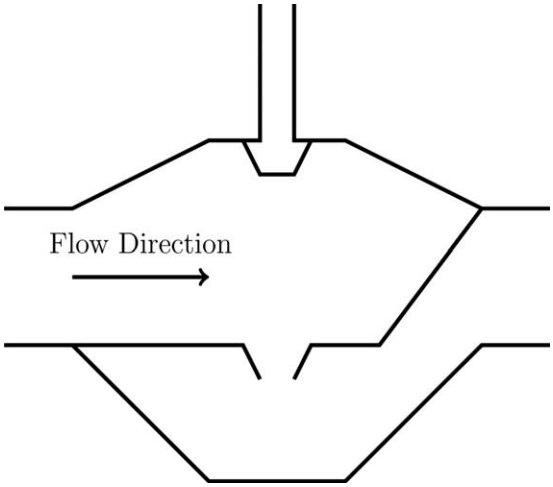


**Figure 4. Schematic depicting a pressure-to-close pneumatic sliding-stem globe valve in the open position.**

**In this work, it is considered that no pressure is being applied to the valve when it is in this position, and the stem position is considered to be at $x_v = 0$ m from the valve's equilibrium, fully open position.**

$$F_f = \sigma_0 z_f + \sigma_1 \frac{dz_f}{dt} + \sigma_2 v_v \tag{39}$$

$$\frac{dz_f}{dt} = v_v - \frac{|v_v|}{g(v_v)} z_f \tag{40}$$

where $\sigma_0$, $\sigma_1$, and $\sigma_2$ are model parameters, $z_f$ is an internal state variable of the friction model, and $g(v_v)$ is a nonlinear function of the valve stem velocity. Although the LuGre model is fundamentally a set of equations that can dynamically capture the effects of friction through the introduction of an appropriately formulated state variable $z_f$, a somewhat physical interpretation of $z_f$ arises if one imagines asperity junctions to behave like contacting bristles that bend against one another until they slip, with stiffness $\sigma_0$ and damping coefficient $\sigma_1$, and $z_f$ representing the average deflection of the bristles. The last term of the friction force is for the viscous friction, with viscous friction coefficient $\sigma_2$. The function $g(v_v)$ aids in defining the Stribeck effect and the friction-velocity characteristics at constant velocity, and for consistency with Refs. 4 and 16, will be taken to be

$$g(v_v) = \frac{1}{\sigma_0}\left[F_C + (F_S - F_C) e^{-(v_v/v_s)^2}\right] \tag{41}$$

where $F_C$ is the Coulomb friction coefficient, $F_S$ is the static friction coefficient, and $v_s$ is the Stribeck velocity. The parameters of the friction model in Eqs. 39–41 are defined in Table 1. The notation in these equations follows that in Eqs. 4 and 5.

**Remark 14.** *The LuGre model is used in this example because its simplicity makes it more suitable for use in MPC than some of the more complex stiction models. Despite its relative simplicity and ability to qualitatively represent a number of friction effects, the LuGre model is neither the most accurate nor the most current friction model available (see, e.g.,* Ref. 18 *for a criticism of its ability to model stiction when an oscillating force with magnitude less than the Coulomb friction level is applied after breakaway, and* Ref. 10 *for a criticism of some of its hysteresis features in presliding, as well as* Refs. 11, 17, and 19 *for more detailed friction models). For the purposes of the example in this article, which demonstrates the general effects that stiction may have on a chemical process and how the incorporation of the dynamics in a model predictive controller can reduce the undesirable effects of stiction, a stiction model that shows qualitatively correct behavior for many scenarios is sufficient.*

*Relating valve position and valve output.* We assume that the valve has a linear installed characteristic[28] so that the valve output is linearly related to the stem position in the following sense

$$u_a = \frac{x_{v,\max} - x_v}{x_{v,\max}} u_{a,\max} \tag{42}$$

**Remark 15.** *The assumption of a linear installed characteristic was made for simplicity of presentation for this example. A variety of other valve characteristics are possible (e.g., an equal percentage or quick opening inherent valve characteristic, or an installed valve characteristic affected by the pressure drop across the valve)[28,46,48,80]; however, the focus of this example is the valve behavior in the presence of stiction, rather than the relationship between the flow and the stem position, so the assumption of a linear installed valve characteristic is considered sufficient. For more information on inherent valve characteristics and how valve installation may affect these characteristics, see* Refs. 28,46, and 80.

*Linear controller model.* In this example, we use a PI controller to regulate the valve output $u_a$ to the set-point $u_m$ set by the EMPC. The PI controller determines the pressure that the valve pneumatic actuation element should apply according to the following equations, which have the form given in Eq. 8

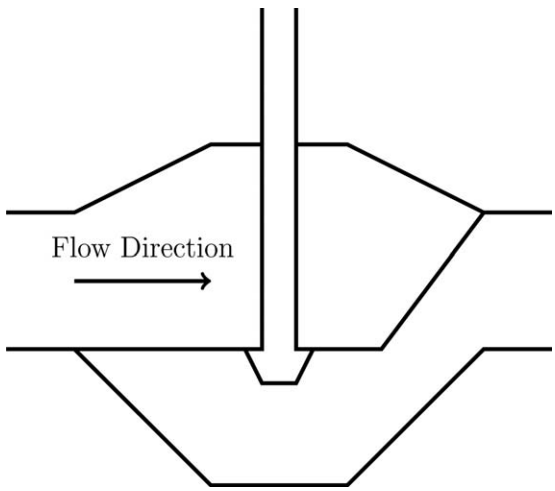


**Figure 5. Schematic depicting a pressure-to-close pneumatic sliding-stem globe valve in the closed position.**

**In this work, the stem position for the closed valve is $x_{v,\max} = 0.1016$ m from the valve's equilibrium, fully open position, and is maintained in this position by the application of pressure to the valve diaphragm.**

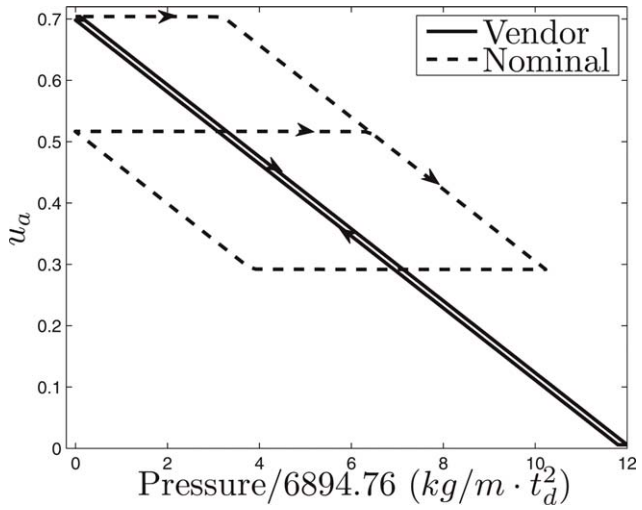


**Figure 6. Comparison of steady-state relationship between $u_a$ and $P$ for the vendor and nominal valve parameters.**

$$P = P_s + 6894.76\left(K_c\left(\frac{u_m - u_a}{u_{a,\max}}\right) + \frac{K_c}{\tau_I}\zeta\right) \tag{43}$$

$$\frac{d\zeta}{dt} = \left(\frac{u_m - u_a}{u_{a,\max}}\right) \tag{44}$$

where $K_c = -12$ and $\tau_I = 0.01$ are the controller gain and integral time, chosen for a fast valve response to a set-point change even with the deadband of the stiction model used in this example. $P_s$ is the steady-state value of the control signal. To ensure that $P$ changes in the correct direction and to prevent the integral error from the previous set-point from impacting the approach to a new set-point once the set-point is changed, we set $P_s$ to the last applied value of $P$ and the value of $\zeta$ to 0 at a set-point change. Combining Eqs. 36–44, we obtain a combined process-valve dynamic model as in Eq. 10, with state $q = [x_1\, x_2\, x_3\, x_4\, x_v\, v_v\, z_f\, \zeta]^T$ and input $u_m$, which we define as $\dot{q} = f_q(x_1, x_2, x_3, x_4, x_v, v_v, z_f, \zeta, u_m)$.

### *Motivation for Actuation Magnitude Constraints*

When the process of Eqs. 36–44 is controlled using EMPC, the EMPC will output a set-point $u_m$ for the valve that controls $u_a$ for each sampling period. The set-point $u_m$ will be used in Eqs. 43 and 44 to determine the pressure that should be applied to the valve to bring it to the requested set-point. Because the dynamics between $u_a$, $u_m$, and $P$ are critical to the EMPC's choice of the value of its optimization variable $u_m$, it is necessary that the dynamics be understood and appropriately constrained to avoid nonphysical situations. This concept will be made clear in this section, which will show that the effect of stiction on the valve dynamics requires the introduction of additional constraints to the EMPC with the form of Eqs. 18f and 18g.

To demonstrate the manner in which stiction changes the dynamics, we first examine the relationship between $u_m$ and $P$ for the open-loop valve in the presence of low stiction and in the presence of significant stiction (the open-loop valve is considered because the parameters $K_c$ and $\tau_I$ in Eqs. 43 and 44 for the closed-loop valve can be adjusted for both the low stiction and significant stiction cases to cause the closed-loop response of the valve output to a set-point change to be rapid). A valve with low stiction can be modeled using the parameters listed in Table 1, with the exception that the values of $F_C$ and $F_S$ in the table are both replaced by 44.48 $\mathrm{kg \cdot m/t_d^2}$. This low stiction valve will be referred to as having "vendor" parameters, in keeping with the terminology used in Ref. 4. The valve parameters listed in Table 1 are those for a valve with stiction that results in deadband at a change of the direction of the velocity of the valve stem (typically, stiction results in slip-jump, but this effect is not apparent for the given model parameters, so in this example, we will assume that the slip-jump is minimal and that the parameters in Table 1 are sufficient to describe stiction in this valve). These are referred to as "nominal" valve parameters.[4]

To determine a relationship between $u_m$ and $P$ that can be used to determine the pressure to apply to the open-loop valve to bring $u_a$ to $u_m$, we start by determining the steady-state relationship between the valve output and the applied pressure for the vendor valve. This relationship is determined by ramping the pressure applied to the valve up and down between 0 $\mathrm{kg/m \cdot t_d^2}$ and 82,737 $\mathrm{kg/m \cdot t_d^2}$ in increments of 69 $\mathrm{kg/m \cdot t_d^2}$ every 0.5 $\mathrm{t_d}$ and recording the value of $u_a$ at the end of every 0.5 $\mathrm{t_d}$, using the Explicit Euler numerical integration method with an integration time step of $10^{-6}$ $\mathrm{t_d}$. The resulting plot of the steady-state value of $u_a$ vs. input pressure is almost linear, as shown in Figure 6. If we assume that $u_m \approx u_a$ for the valve because stiction is low so the valve output should track its set-point well, we obtain the following relationship between $u_m$ and $P$ for the vendor valve using a least-squares optimization on the vendor valve data (neglecting the initial transient) shown in Figure 6

$$u_m = -\frac{0.05864}{6894.76} * P + 0.70391 \tag{45}$$

We now assume that we have a series of desired set-points $u_m$ that we would like to achieve for the open-loop valve with significant stiction (nominal valve). We investigate whether the $u_m - P$ relationship developed for the vendor valve is applicable for the nominal valve by developing the $u_a - P$ relationship when the pressure value calculated from Eq. 45 is applied to the nominal valve to attempt to achieve the desired value of $u_m$. Accordingly, we ramp the set-point $u_m$ up and down between 0.1042 and 0.7042 in increments of 0.01 every

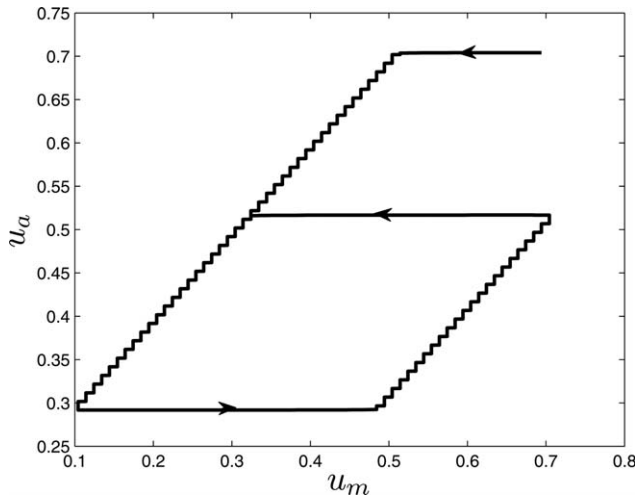


**Figure 7. Open-loop values of $u_a$ and $u_m$ for the nominal valve.**

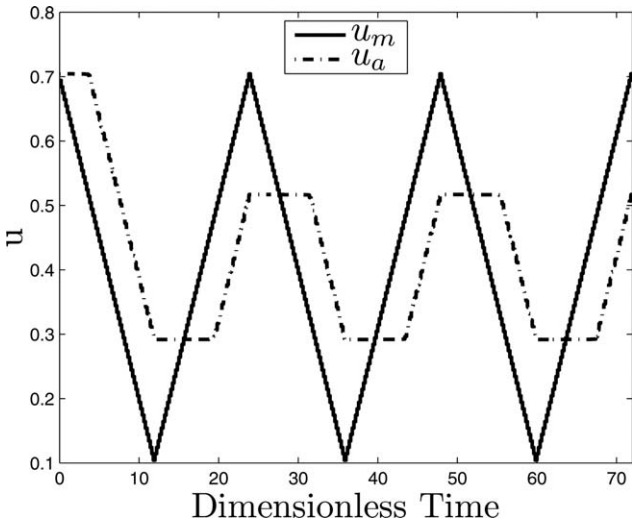


**Figure 8. Open-loop values of $u_a$ and $u_m$ with time for the nominal valve.**

0.5 $t_d$ and record the value of $u_a$ at the end of every 0.5 $t_d$, again using the Explicit Euler numerical integration method with an integration time step of $10^{-6}$ $t_d$ (the Explicit Euler numerical integration method with an integration time step of $10^{-6}$ $t_d$ was used for all simulations of the nominal valve in this "Motivation for Actuation Magnitude Constraints" Section). The resulting $u_a - P$ relationship can no longer be described as one linear relation, but two that depend on whether the pressure is being increased or decreased, and the deadband at a velocity change is visible in Figure 6. In addition, it can be observed from the figure that because of the effect of stiction on the $u_a - P$ relationship, there are certain flow rates that can be achieved with a positive pressure for the vendor valve that would require a negative pressure for the nominal valve, which is physically not possible to achieve. This is the first hint that to compensate for stiction, additional constraints of the form of Eqs. 18f and 18g will need to be added to the EMPC to prevent physically unrealizable set-points from being requested.

As shown in Figure 6, the linear relationship between $u_m$ and $P$ developed in Eq. 45 is not sufficient to control a valve subject to stiction. Further evidence of this comes from ramping the set-point $u_m$ of the nominal open-loop valve up and down between 0.1042 and 0.7042 in increments of 0.01 every sampling period of length $\Delta = 0.2$ $t_d$ and determining the pressure to apply to the valve from Eq. 45. The dynamic response (i.e., not steady-state; this is the reason for the step-like quality of the trajectories) of the valve output to these set-point changes is shown in Figures 7 and 8. Figure 7 shows the insufficiency of Eq. 45 to determine the pressure value that should be applied to the valve for a desired $u_m$ because it shows that for this sticky valve, $u_a$ does not effectively track $u_m$ (the $u_a - u_m$ plot in Figure 7 is not linear). This is further emphasized in Figure 8, which also shows the deadband when $u_m$ begins to change in the opposite direction to that in which it was changing previously. This demonstrates that a different relationship between $u_m$ and $P$ is needed to control the nominal valve than that provided by Eq. 45 to ensure good set-point tracking.

In the proposed method, the linear controller of Eqs. 43 and 44 is used to improve the set-point tracking performance of $u_a$. To demonstrate that this does indeed improve the set-point tracking, we ramp the set-point $u_m$ to the nominal valve in closed-loop with the linear controller in Eqs. 43 and 44, again ramping it up and down between 0.1042 and 0.7042 in increments of 0.01 every $\Delta = 0.2$ $t_d$. The dynamic response of the valve is shown in Figures 9 and 10 which show that the $u_a - u_m$ relationship is close to linear under the linear controller, and that $u_a$ is able to closely track $u_m$ in time and is quickly able to overcome the deadband caused by stiction. However, despite its benefit in providing good set-point tracking performance, the use of Eqs. 43 and 44 does not ensure that the value of $P$ requested will not become negative. This is demonstrated in Figures 11 and 12, which plot the dynamic response of the closed-loop valve to eight set-point changes ($u_m$=0.35, 0.2, 0.35, 0.2, 0.3, 0.4, 0.5, and 0.6) each held for $\Delta = 0.2$ $t_d$ when initialized from the fully open position (i.e., $u_a$=0.7042, $P_s$=0 $kg/m \cdot t_d^2$, $x_v$=0 m, $v_v$=0 $m/t_d$, $z_f$= 0 m initially). The results in Figure 11 again show that the PI control law developed in Eqs. 43 and 44 helps the valve to effectively track its set-points even when there is deadband because the direction of the valve stem movement changes. However, the results of Figure 12 show that the good set-point tracking can only be achieved when the pressure is able to adjust as necessary, including becoming negative, which is physically impossible. From Figures 11 and 12, it can be deduced that if the pressure is saturated at 0 $kg/m \cdot t_d^2$ when a lower pressure is requested, the valve output would not be able to reach all of the set-points in this simulation. This indicates that when the control law of Eqs. 43 and 44 is used, the constraints of the EMPC need to ensure that the pressure does not become negative at the set-points it requests, because the control law itself does not ensure this.

**Remark 16.** *In this section, ramping of set-point changes was used to demonstrate the good set-point tracking performance of the PI controller in Eqs. 43 and 44. If the ramping of the set-point changes is too rapid, however, the*

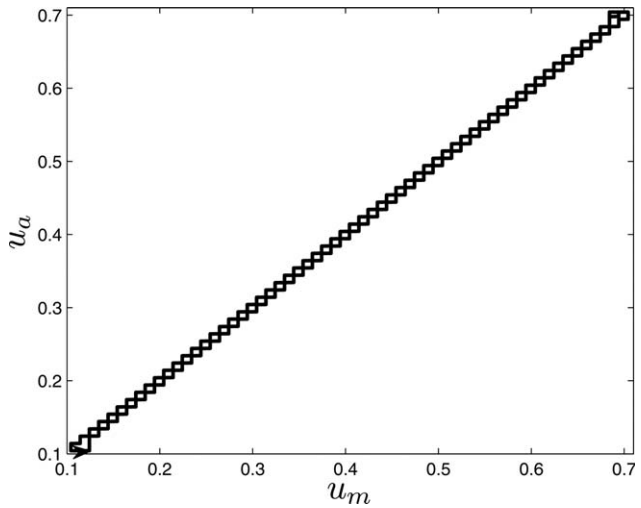


**Figure 9. Closed-loop values of $u_a$ and $u_m$ for the nominal valve under PI control.**

**The plot depicts that $u_a$ increases with increasing $u_m$ and decreases with decreasing $u_m$ when the value of $u_m$ is changed by 0.01 every $\Delta$. The arrow in the lower left corner of the plot shows the direction in which the increasing and decreasing steps in the plot are traversed.**

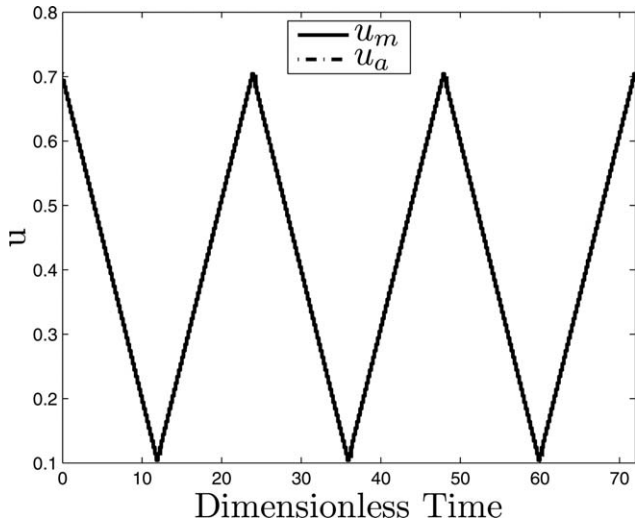


**Figure 10. Closed-loop values of $u_a$ and $u_m$ with time for the nominal valve under PI control.**

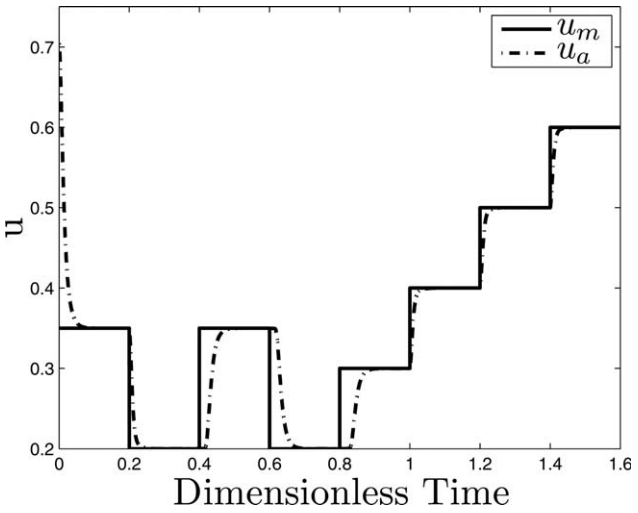


**Figure 11. Closed-loop values of $u_a$ and $u_m$ with time for the nominal valve under PI control for several set-point changes.**

*closed-loop control valve under PI control may be destabilized.*

**Remark 17.** *The constraint* $P \geq 0$ $\mathrm{kg/m \cdot t_d^2}$ *was developed for the EMPC in this section to ensure that the set-points calculated by the EMPC are physically realizable (i.e., that they do not require the pressure to become negative for* $u_a$ *to meet* $u_m$*). Based on the plots presented in this section, other methods for handling this scenario could be considered as well. For example, based on Figure 6, another method for preventing negative pressures for this example may be to decrease the range of allowable values of* $u_m$ *as stiction worsens such that the allowable values of* $u_m$ *always correspond to positive pressures. However, it may be difficult to determine what the new bound on* $u_m$ *should be without doing an offline test to generate data like that in Figure 6, and the valve stiction may continue to worsen with time, meaning that new ranges for* $u_m$ *may need to be determined throughout time. In addition, because the profit from EMPC may be improved by allowing operation over a larger region of state-space, it is not desirable to choose extremely conservative bounds on* $u_m$ *to avoid the calculation of set-points that would require negative pressures because that may lower profit below that which could be realized. Motivated by these considerations, for the EMPC in this example, we set the constraint of Eq. 18g in our proposed MPC compensation strategy to be a constraint that the actuator pressure must never become negative.*

**Remark 18.** *We note that the basic relationships between* $u_m$*,* $u_a$*, and P presented in this section are well-known; for example, one can find plots similar to those in Figures 6–8 in* Refs. 3–5*. In addition, it is well-known that control of the valve position may help to improve the response of a valve in the presence of valve nonlinearities (e.g.,* Ref. 5 *suggests a control law to bring the valve position to its set-point in the presence of stiction, and* Ref. 33 *states that valve positioners are often able to improve a valve's response if it exhibits deadband). The results in this section are novel, however, because they present the dynamic plots of the open and closed-loop valve responses as an analysis tool useful for the design of an MPC with appropriate constraints for stiction compensation and show how this analysis can be carried out using plots of this type. Furthermore, this discussion is not meant to be applicable only to this example, but to suggest the type of thinking and analysis that may need to go into the design of the proposed MPC for other processes.*

### *Proposed MPC Formulation*

In this section, we describe the performance of an EMPC formulation meeting the form of our proposed MPC stiction compensation strategy in Eq. 18 with the process-valve model of Eqs. 36–44 and the constraint that $P \geq 0$ $\mathrm{kg/m \cdot t_d^2}$ at all times.

The control objective is to maximize the yield of the product ethylene oxide. The yield of ethylene oxide between the initial and final times of the plant operation ($t_0$ and $t_f$) is defined as

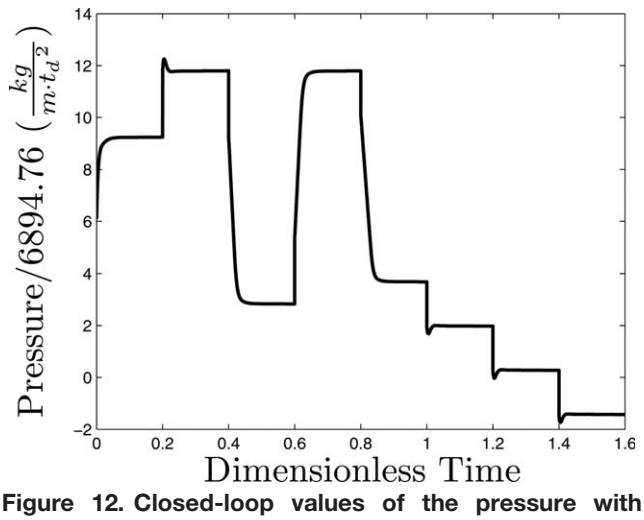


**Figure 12. Closed-loop values of the pressure with time for the nominal valve under PI control for several set-point changes.**

$$Y(t_f)=\frac{\int_{t_0}^{t_f} u_a(\tau)x_3(\tau)x_4(\tau)d\tau}{\int_{t_0}^{t_f} u_a(\tau)C_e d\tau} \tag{46}$$

However, we assume that the volumetric flow rate of the inlet stream is bounded such that between $t_0$ and $t_f$, the following integral holds

$$\frac{C_e}{t_f-t_0}\int_{t_0}^{t_f} u_a(\tau)d\tau=0.175 \tag{47}$$

Combining Eqs. 46 and 47, the objective of the EMPC becomes the maximization of the time integral of the stage cost $L_{\mathrm{MPC}}$, where $L_{\mathrm{MPC}}$ is defined as follows

$$L_{\mathrm{MPC}}=u_a(\tau)x_3(\tau)x_4(\tau) \tag{48}$$

The input $u_a$ is physically bounded between the flow rates at the maximum and minimum valve openings as follows

$$u_{a,\min} \le u_a \le u_{a,\max} \tag{49}$$

with $u_{a,\min}=0$ (valve fully closed) and $u_{a,\max}=0.7042$ (valve fully open). The value of $u_a$ is computed using the actuator layer equations in Eqs. 37–44.

We assume that the only data available to aid in choosing the allowable range of valve set-points $u_m$ that the EMPC calculates is the vendor data in Figure 6. Thus, we assume that the bounds developed for the EMPC include set-points that can only be met with negative pressures by the nominal valve, although they can be met with positive pressures by the vendor valve. The set-points $u_m$ are thus restricted as follows

$$u_{m,\min} \le u_m \le u_{m,\max} \tag{50}$$

with $u_{m,\min}=0.0704$ and $u_{m,\max}=0.7042$ (the minimum value of $u_m$ is greater than 0 because we assume that we want to avoid fully closing the valve for this process). Physically, the pressure applied to the valve diaphragm cannot drop below $0\ \mathrm{kg/m\cdot t_d^2}$.

For this example, the optimization variable $u_a$ does not have a large effect on the process economics, with the result that the process yields under steady-state operation and under EMPC operation are approximately equal in the long term when the valve has no stiction. Thus, we emphasize that the choice to use EMPC for this example is primarily driven, as previously noted, by the ability of EMPC to promote time-varying operation such that it computes set-points at the bounds of what is physically possible to maximize the process profit and thus effectively illustrates the advantages of including the constraint on the actuation magnitude (pressure). Furthermore, the profitability of EMPC over steady-state operation for a variety of processes has been well-documented in the literature (see, e.g., Refs. 57 and 81), including for the present example when two actuators are used as in Ref. 45, and is not the focus of this work. However, it is noted that the process in the absence of stiction or valve dynamics has a steady-state yield of 6.63% over 468 $\mathrm{t_d}$ and a yield of 32.22% over 2 $\mathrm{t_d}$ when initiated from $[x_{1I}\ x_{2I}\ x_{3I}\ x_{4I}]^T=[0.997\ 1.264\ 0.209\ 1.004]^T$. This shows that for the two operating periods considered in this study, the effect of the transient is very strong because the average steady-state yield is much larger over the 2 $\mathrm{t_d}$ considered in this study than it is after a longer time period.

To achieve the above objectives while countering stiction, we develop an EMPC, termed EMPC $-$ $A$, that incorporates actuator dynamics to aid in stiction compensation and maximizes the yield of ethylene oxide subject to the integral material constraint and constraints on the allowable values of the valve output, valve set-point, and actuator output to prevent nonphysical situations. This EMPC solves the following optimization problem

$$\min_{u_m(t)\in S(\Delta)} -\int_{t_k}^{t_{k+N_k}} \tilde{u}_a(\tau)\tilde{x}_3(\tau)\tilde{x}_4(\tau)\,d\tau \tag{51a}$$

$$\text{s.t. } \dot{\tilde{q}}(t)=f_q(\tilde{q}(t),u_m(t)) \tag{51b}$$

$$\tilde{q}(t_k)=q(t_k) \tag{51c}$$

$$0 \le \tilde{u}_a(t) \le 0.7042,\ \forall\, t\in[t_k,t_{k+N}] \tag{51d}$$

$$0.0704 \le u_m(t) \le 0.7042,\ \forall\, t\in[t_k,t_{k+N}) \tag{51e}$$

$$\tilde{P}(t) \ge 0,\ \forall\, t\in[t_k,t_{k+N}] \tag{51f}$$

$$\int_{t_k}^{t_{k+N_k}} \tilde{u}_a(\tau)d\tau+\int_{(j-1)t_p}^{t_k} u_a^*(\tau)d\tau=\frac{0.175t_p}{C_e} \tag{51g}$$

where the cost function in Eq. 51a represents the total yield of ethylene oxide throughout the prediction horizon when the material constraint is met, and Eq. 51g is the method for implementing the integral material constraint by constraining the value of $u_a$ to meet the material constraint in each operating period. Equation 51g states that the time-average value of the sum of the predicted valve outputs $\tilde{u}_a$ plus the previously applied valve outputs $u_a^*$ must be no greater than $\frac{0.175}{C_e}$ over the $j$th operating period ($j=1,2,\ldots$). A shrinking prediction horizon is used, such that the prediction horizon $N_k=5$ at the beginning of an operating period of length $t_p=1\ \mathrm{t_d}$ ($\Delta=0.2\ \mathrm{t_d}$) but is decremented by 1 at each subsequent sampling time in the operating period. The use of this shrinking horizon allows the integral material constraint of Eq. 47 to be implemented in Eq. 51g. The state constraints in Eqs. 51d and 51f were enforced every two integration steps. Because this process has an asymptotically stable steady-state, the Lyapunov-based constraints of Eqs. 18l and 18m were not considered. The dynamic equation in Eq. 51b was integrated within the EMPC using the Explicit Euler numerical integration method with an integration step of $h_A=10^{-6}\ \mathrm{t_d}$. Centered finite difference approximations of derivatives required for the solution of the optimization problem were obtained by perturbing the optimization variables by $10^{-6}$.

For comparison with EMPC $-$ $A$, we also introduce an EMPC that does not include the valve dynamics, which will be referred to as EMPC $-$ $B$, formulated as follows

$$\min_{u_m(t)\in S(\Delta)} -\int_{t_k}^{t_{k+N_k}} u_m(\tau)\tilde{x}_3(\tau)\tilde{x}_4(\tau)\,d\tau \tag{52a}$$

$$\text{s.t. } \dot{\tilde{x}}(t)=f(\tilde{x}(t),u_m(t)) \tag{52b}$$

$$\tilde{x}(t_k)=x(t_k) \tag{52c}$$

$$0.0704 \le u_m(t) \le 0.7042,\ \forall\, t\in[t_k,t_{k+N}) \tag{52d}$$

$$\int_{t_k}^{t_{k+N_k}} u_m(\tau)d\tau+\int_{(j-1)t_p}^{t_k} u_m^*(\tau)d\tau=\frac{0.175t_p}{C_e} \tag{52e}$$

where the notation in Eq. 52b signifies that $u_a$ in Eqs. 36a–36d is replaced by $u_m$ in the model used to predict the process states within EMPC $-$ $B$. Numerical integration of the dynamic equation in Eq. 52b was performed using the Explicit

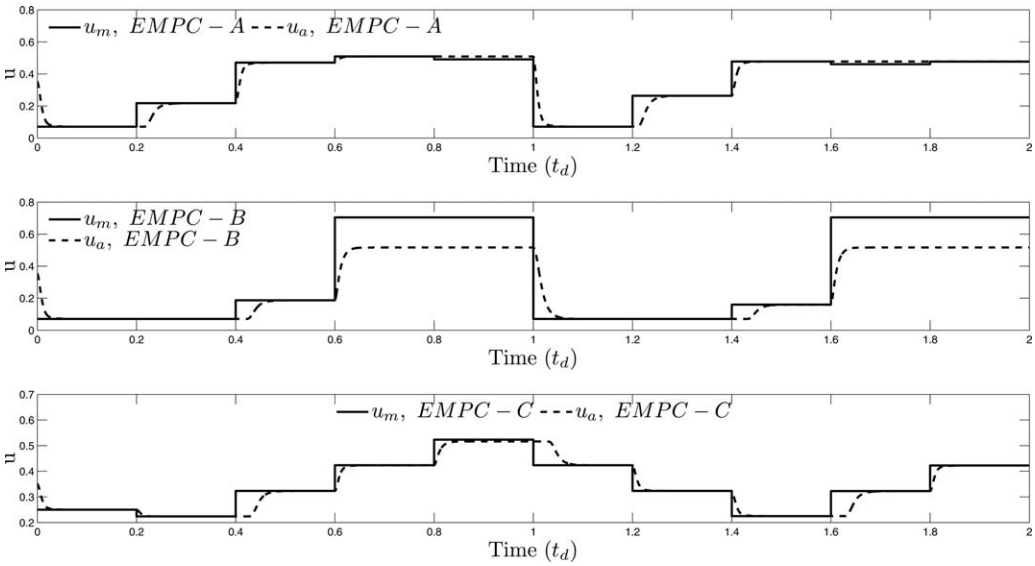


**Figure 13. Valve output set-points $u_m$ (solid trajectories) and actual valve outputs $u_a$ (dashed trajectories) throughout two operating periods for EMPC − *A*, EMPC − *B*, and EMPC − *C*.**

Euler method with an integration time step of $h_B=10^{-4}$ $t_d$. Centered finite difference approximations of derivatives required for the solution of the optimization problem were obtained by perturbing the optimization variables by $10^{-4}$.

A third EMPC, EMPC − *C*, was also developed with the form of EMPC − *B* but with rate of change constraints added, for reasons that will be clarified below. EMPC − *C* solves the following optimization problem

$$\min_{u_m(t)\in S(\Delta)} -\int_{t_k}^{t_{k+N_k}} u_m(\tau)\tilde{x}_3(\tau)\tilde{x}_4(\tau)\,d\tau \tag{53a}$$

$$\text{s.t. } \dot{\tilde{x}}(t)=f(\tilde{x}(t),u_m(t)) \tag{53b}$$

$$\tilde{x}(t_k)=x(t_k) \tag{53c}$$

$$0.0704 \le u_m(t) \le 0.7042,\ \forall\, t\in[t_k,t_{k+N}) \tag{53d}$$

$$\int_{t_k}^{t_{k+N_k}} u_m(\tau)d\tau+\int_{(j-1)t_p}^{t_k} u_m^*(\tau)d\tau=\frac{0.175t_p}{C_e} \tag{53e}$$

$$|u_m(t_k)-u_m^*(t_{k-1}|t_{k-1})| \le \gamma \tag{53f}$$

$$|u_m(t_j)-u_m(t_{j-1})| \le \gamma,\ j=k+1,\ldots,k+N_k-1 \tag{53g}$$

where $\gamma$ in Eqs. 53f and 53g is a constant that defines the change in $u_m$ that will be accepted between sampling periods. In the following simulations, $\gamma=0.1$. Equation 53b was numerically integrated using the Explicit Euler numerical integration method with an integration step size of $h_C=10^{-4}$ $t_d$. Centered finite difference approximations of derivatives required for the solution of the optimization problem were obtained by perturbing the optimization variables by $10^{-4}$.

Outside of EMPC − *A*, EMPC − *B*, and EMPC − *C*, the actual process was simulated using Eqs. 36–44 with an Explicit Euler integration step size of $h=10^{-6}$ $t_d$, with the pressure saturated at 0 $kg/m\cdot t_d^2$ if a lower pressure was requested ($u_a$ would have been saturated at $u_{a,\min}$ or $u_{a,\max}$ if those values were exceeded, but neither of these extremes were violated in these simulations). All three EMPC's used $t_p=1$ $t_d$, $\Delta=0.2$ $t_d$, and simulated the results for two operating periods. They were initiated from the point $q_I=[0.997\ 1.264\ 0.209\ 1.004\ 0.051\ 2.000\times10^{-6}\ 1.426\times10^{-5}\ 0]^T$, where the process states are dimensionless and the states of the actuator layer have SI units except for a dimensionless time unit as in Table 1, and the initial value of the steady-state pressure is $P_{s,I}=63,713$ $kg/m\cdot t_d^2$. All optimizations were performed using the open-source nonlinear interior point optimization solver Ipopt[82] and were coded in the C++ programming language. The Ipopt convergence tolerance for optimization termination was set to $10^{-10}$ for EMPC − *A*, and to $10^{-8}$ for EMPC − *B* and EMPC − *C*. Simulations were carried out on a 2.40 GHz Intel Core 2 Quad CPU Q6600 on a 64-bit Windows 7 Professional operating system with 4.00 GB of RAM.

Figures 13 and 14 show the values of $u_a$, $u_m$, and $P$ for the valve with time when the system of Eqs. 36–44 is controlled by EMPC − *A* and EMPC − *B*. These figures show that the inclusion of valve dynamics and actuation magnitude constraints in EMPC causes EMPC − *A* to calculate lower set-points than EMPC − *B*, which allows the valve output to track the EMPC-requested set-points throughout the two operating periods, even when the pressure drops, because EMPC − *A* is aware of the limitations of the pneumatic actuation and thus calculates set-points that the valve output can reach (it is noted that there are two small set-point changes in Figure 13 that $u_a$ for EMPC − *A* does not track; the reason for this will be explained further below, but the overall trend that $u_a$ tracks $u_m$ well under EMPC − *A* can be deduced from Figure 13). Figures 13 and 14 show that when the actuator dynamics are not included in EMPC and stiction develops with time such that the pressure-flow rate relationship is altered, the valve output is not able to track the EMPC − *B* set-points because EMPC − *B* calculates set-points for which the pressure would need to drop to negative values to allow the valve to move enough to reach them (because this is physically impossible, the pressure under EMPC − *B* saturates at its minimum value of 0 $kg/m\cdot t_d^2$ for four sampling periods, although the pressure under EMPC − *A* does not because the set-points calculated by EMPC − *A* are reachable). The inability of the valve to reach the set-points calculated by EMPC − *B* causes the EMPC − *B* optimization problem to become infeasible in the last two sampling periods of each operating period and causes EMPC − *B* to be unable to meet the integral constraint (it cannot use all available material; the value of the integral constraint in Eq. 47 calculated for each operating period (i.e.,

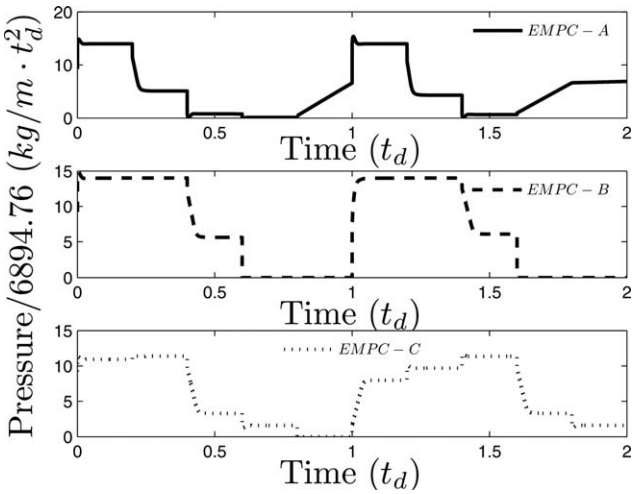


**Figure 14. Actuator pressure applied to valve stem throughout two operating periods for EMPC − *A* (solid trajectory), EMPC − *B* (dashed trajectory), and EMPC − *C* (dotted trajectory).**

between $(j-1)t_p$ and $jt_p$, $j = 1, 2$, instead of between $t_0$ and $t_f$) is approximately 0.133, which is 24% less than the required value of 0.175). The yield of EMPC − *A* throughout two operating periods according to Eq. 46 is 32.4%, while that of EMPC − *B* according to Eq. 46 is 35.1%. This at first appears to suggest that EMPC − *B* out-performs EMPC − *A* economically; however, because EMPC − *B* did not meet a hard constraint of the process, the yield that it achieved without meeting this constraint cannot be compared with the yield of a process that did meet the constraint. Thus, no further discussion of yields under the various EMPC's will be pursued, and the discussion will focus on the degree to which the various formulations ensure that the process constraints are satisfied. In contrast to EMPC − *B*, EMPC − *A* is feasible in both operating periods.

Despite the advantages of using EMPC − *A* rather than EMPC − *B* to ensure that all process constraints are met, the computational burden of EMPC − *A* due to the enforcement of the constraints on the pressure and on $u_a$ at every other integration step $h_A = 10^{-6}$ $t_d$ within the EMPC is much larger than that for EMPC − *B*. In an actual plant, this computation time increase could prohibit the use of EMPC − *A* if the process has fast dynamics such that a short sampling time is required for effective control. However, the input rate of change constraints discussed in this article for the design of an MPC incorporating nonlinear valve dynamics may be considered for use in EMPC − *B* to minimize the large jumps in $u_m$ that cause EMPC − *B* to be unable to meet the material constraint at the end of the operating periods but without adding much computation time. Thus, we demonstrate the use of input rate of change constraints and how they affect the trajectories of $u_m$, $u_a$, and $P$ using EMPC − *C*. Figures 13 and 14 show these trajectories and show that the addition of the input rate of change constraints to EMPC − *B* to form EMPC − *C* significantly improves the set-point tracking performance compared to EMPC − *B*. In contrast to EMPC − *B*, for which four of the set-points were not reachable and caused significant offset, there is only one set-point calculated by EMPC − *C* in Figure 13 for which offset is observed, and the offset is much smaller than those for EMPC − *B*. In addition, the pressure in Figure 14 only saturates at its minimum value for one sampling period under EMPC − *C*, instead of the four during which it saturates under EMPC − *B*. Although EMPC − *C* is infeasible for three sampling periods (the last two sampling periods of the first operating period and the last sampling period of the second operating period) and the integral constraint is not met at the end of either operating period, the degree to which the integral constraint is violated is significantly less than under EMPC − *B* (the integral constraint is 0.171 at the end of the first operating period and 0.172 at the end of the second under EMPC − *C*, such that in each operating period, it is only about 2% less than the required value of 0.175). In addition, the computation time of EMPC − *C* is, as for EMPC − *B*, much lower than that for EMPC − *A* owing to the use of a lower-order model than EMPC − *A*. The rate of change constraints were added to EMPC − *C* in an *ad hoc* fashion and are not guaranteed to reduce the negative effects of stiction on the controller performance, but the positive impact that they had on the process performance does indicate the breadth of constraints that could be considered to combat the effects of stiction with both the proposed MPC and also with MPC's for processes that cannot fully incorporate the proposed method due to computation time constraints.

Figures 15 and 16 show the closed-loop process and actuator layer states under EMPC − *A*, EMPC − *B*, and EMPC − *C*. Figure 15 shows that the process state trajectories are not drastically affected by the differences between the trajectories of $u_a$ under the three EMPC's, which contributes to the fact that the focus of this example is not on the profitability of the proposed EMPC compared to the other methods, but rather on its ability to meet the constraints of the process when the valve is affected by stiction. The plot of the controller state $\zeta$ in Figure 16 shows the manner in which the integral term of the controller is affected by the different EMPC formulations. In EMPC − *B*, the integral term becomes large in the sampling periods in which the EMPC cannot reach its set-points. This plot also shows the benefits of resetting the value of $\zeta$ to zero at each set-point change so that, for example, the value of $\zeta$ for EMPC − *B* at the beginning of the second operating period is not wound up from the integration of this state at the end of

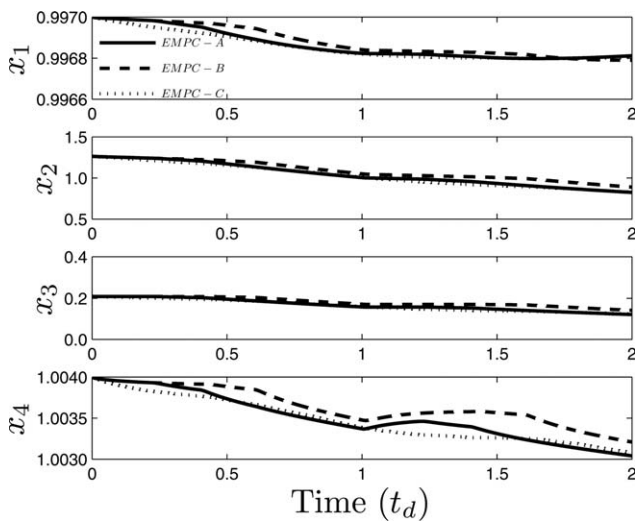


**Figure 15. Closed-loop process states $x_1$, $x_2$, $x_3$, and $x_4$ throughout two operating periods under EMPC − *A* (solid trajectories), EMPC − *B* (dashed trajectories), and EMPC − *C* (dotted trajectories).**

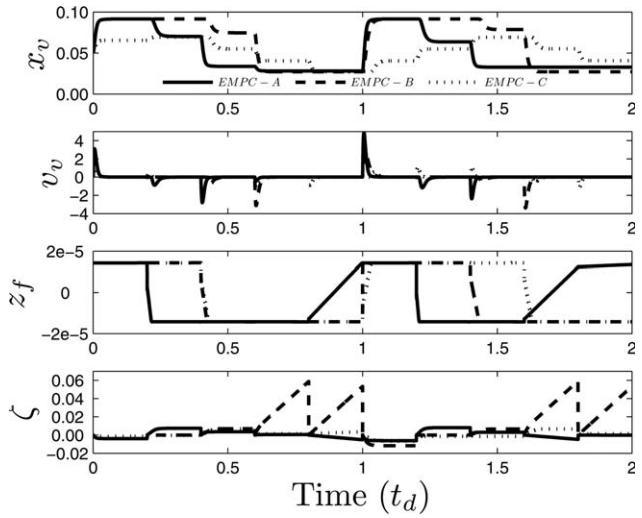


**Figure 16. Closed-loop actuator layer states $x_v$, $v_v$, $z$, and $\zeta$ throughout two operating periods under EMPC – *A* (solid trajectories), EMPC – *B* (dashed trajectories), and EMPC – *C* (dotted trajectories).**

the first operating period. In addition, the plot shows that the inclusion of the actuator dynamics and constraints on the pressure in EMPC $-$ $A$ and rate of change constraints in EMPC $-$ $C$ prevent the integral term from becoming large because they ensure that the set-points can be met or (in the case of EMPC $-$ $C$) reached closely enough so that the integral term does not reach large values. In addition, the increase in $\zeta$ at a direction change of the velocity to allow the pressure to overcome the deadband is visible in this plot as well.

The trajectories in Figures 13, 14, and 16 show the relationships between the physical states $x_v$ and $v_v$ of the valve and the valve output and pressure applied to the valve for the process under EMPC $-$ $A$, EMPC $-$ $B$, and EMPC $-$ $C$. Because the value of $u_a$ is an explicit function of $x_v$, changes in $u_a$ occur when $x_v$ changes. A comparison of the trajectories of $x_v$ and $u_a$ with the values of $P$ for EMPC $-$ $A$ shows the deadband where the pressure is increasing but the values of $x_v$ and $u_a$ do not change much because the error (and thus $\zeta$) is not large enough to cause much stem movement for the small set-point changes toward the end of the first and second operating periods of the EMPC. The set-point changes in EMPC $-$ $B$ and EMPC $-$ $C$ are all significant enough that the deadband is overcome within a sampling period. The velocity $v_v$ for all three EMPC's is nonzero when $x_v$ and thus $u_a$ are changing, but is zero when $u_a$ reaches $u_m$ and the friction force balances the pressure and spring forces on the valve.

The trajectories of $z_f$ in Figure 16 show that when deadband is encountered, the state $z_f$ is driven through zero. This is consistent with the physical visualization of $z_f$ suggested by the authors of the LuGre model,[16] which related it to the average deflection of theoretical bristles on two contacting surfaces, whose bending caused friction. It would be expected that bristles would be deflected from an equilibrium (zero) location corresponding to the starting position of the valve when the stem position first begins to move in a given direction. In addition, it is necessary for continuity of the friction force in Eq. 39 that the value of $z_f$ approach this zero value in a dynamic fashion, rather than abruptly. The passing of $z_f$ through zero at a change in the direction of set-point changes allows the friction force of Eq. 39 to change direction so that it continues to be in the direction opposite the applied force.

We now address the fact that EMPC $-$ $A$ calculated set-points that are not reachable (see Figure 13) although it could predict the dynamics of the valve with respect to the set-point changes. Stiction is often noticeable when pressure is applied to a valve, but the valve stem does not move because the opposing friction force is significant. This phenomenon is exhibited during the two set-point changes for EMPC $-$ $A$ that the valve output does not track. Due to the small set-point reversals in $u_m$ requested by EMPC $-$ $A$ at the end of the first and second operating periods, the value of the pressure applied to the valve according to Eqs. 43 and 44 does not change quickly as the error between $u_m$ and $u_a$ (and thus $\zeta$) is low. However, although the valve is considered to be stuck at this time, as the pressure changes, the dynamics in Eqs. 37–41 cause the stem position and velocity (in addition to $z_f$) to continue to change, although slowly. It is because of this effect that EMPC $-$ $A$ calculates set-points that it cannot reach; it does so to manipulate the numerical results such that the valve stem and thus output would move just enough in the sampling periods in which unreachable set-points are calculated to allow all constraints to be met, including the integral constraint. While this suggests that the results are dependent on the friction model used, it also shows that including the friction model within the EMPC allows the EMPC to make smart set-point choices that are not necessarily intuitive.

To demonstrate the robustness of the proposed approach to disturbances and plant-model mismatch, the process of Eqs. 36–44 was controlled by EMPC $-$ $A$ and was simulated with different levels of bounded Gaussian white noise in the process and actuator states, and the closed-loop stability of the process under EMPC $-$ $A$ was found to be robust with respect to the different noise levels. In addition, when the process was simulated with noise in the process states with standard deviation $\sigma_w = [0.1\ 300\ 60\ 0.4\ 0\ 0\ 0\ 0]^T$ and bound $\theta = [0.3\ 900\ 180\ 1.2\ 0\ 0\ 0\ 0]^T$ (this standard deviation and bound on the noise were chosen because they provided a meaningful perturbation to the process states when added to the right-hand side of Eqs. 36a–36d), the integral material constraint was met in both operating periods.

## Conclusions

In this work, we showed that MPC can be used to compensate for the effects of stiction by including detailed valve dynamics for sticky valves in addition to constraints on the rate of change of inputs and the actuation magnitude. Although the focus of the proposed method was on stiction compensation, it could be considered for ameliorating the negative effects of other nonlinear valve behavior, such as backlash resulting in deadband. We defined the process-valve model in general terms so that the proposed approach could be adapted to a variety of valve types. The flexibility of the MPC-based stiction compensation strategy, which allows it to incorporate a variety of cost functions or constraints to reduce tracking offset or oscillations in control loops, was discussed. In addition, closed-loop stability and feasibility of the MPC optimization problem including Lyapunov-based stability constraints were proven for a sufficiently small sampling period. Using a chemical process example, we showed how constraints can be developed for the MPC for stiction compensation and demonstrated that this MPC can result in better valve

layer set-point tracking and constraint satisfaction than an MPC that does not account for stiction.

## Acknowledgment

Financial support from the National Science Foundation and the Department of Energy is gratefully acknowledged.

## Literature Cited


1. Desborough L, Miller R. Increasing customer value of industrial control performance monitoring-Honeywell's experience. In *AIChE Symposium Series*. New York: American Institute of Chemical Engineers, 2002:172–192.
2. Nallasivam U, Babji S, Rengaswamy R. Stiction identification in nonlinear process control loops. *Comput Chem Eng* 2010;34: 1890–1898.
3. Choudhury MAAS, Thornhill NF, Shah SL. Modelling valve stiction. *Control Eng Pract* 2005;13:641–658.
4. Garcia C. Comparison of friction models applied to a control valve. *Control Eng Pract*. 2008;16:1231–1243.
5. Kayihan A, Doyle FJ III. Friction compensation for a process control valve. *Control Eng Pract*. 2000;8:799–812.
6. Choudhury MAAS. Plantwide oscillations diagnosis-current state and future directions. *Asia-Pac J Chem Eng*. 2011;6:484–496.
7. Choudhury MAAS, Jain M, Shah SL. Stiction-definition, modelling, detection and quantification. *J Process Control*. 2008;18:232–243.
8. Brásio ASR, Romanenko A, Fernandes NCP. Modeling, detection and quantification, and compensation of stiction in control loops: The state of the art. *Ind Eng Chem Res*. 2014;53:15020–15040.
9. Armstrong-Hélouvry B, Dupont P, Canudas de Wit C. A survey of models, analysis tools and compensation methods for the control of machines with friction. *Automatica*. 1994;30:1083–1138.
10. Swevers J, Al-Bender F, Ganseman CG, Prajogo T. An integrated friction model structure with improved presliding behavior for accurate friction compensation. *IEEE Trans Autom Control*. 2000;45: 675–686.
11. Al-Bender F, Lampaert V, Swevers J. A novel generic model at asperity level for dry friction force dynamics. *Tribol Lett*. 2004;16: 81–93.
12. Wang J, Zhang Q. Detection of asymmetric control valve stiction from oscillatory data using an extended Hammerstein system identification method. *J Process Control*. 2014;24:1–12.
13. Olsson H, Åström KJ, Canudas de Wit C, Gäfvert M, Lischinsky P. Friction models and friction compensation. *Eur J Control*. 1998;4: 176–195.
14. Dahl PR. *A Solid Friction Model*. Technical Report TOR-0158(3107-18)−1. El Segundo, CA: Aerospace Corporation, 1968.
15. Olsson H. *Control Systems with Friction*. PhD Thesis. Lund Institute of Technology, 1996.
16. Canudas de Wit C, Olsson H, Åström KJ, Lischinsky P. A new model for control of systems with friction. *IEEE Trans Autom Control*. 1995;40:419–425.
17. Lampaert V, Swevers J, Al-Bender F. Modification of the Leuven integrated friction model structure. *IEEE Trans Autom Control*. 2002;47:683–687.
18. Dupont P, Armstrong B, Hayward V. Elasto-plastic friction model: contact compliance and stiction. In *Proceedings of the American Control Conference*. Chicago, IL, 2000:1072–1077.
19. Lampaert V, Al-Bender F, Swevers J. A generalized Maxwell-Slip friction model appropriate for control purposes. In *Proceedings of the International Conference on Physics and Control*. St. Petersburg, Russia, 2003:1170–1177.
20. Stenman A, Gustafsson F, Forsman K. A segmentation-based method for detection of stiction in control valves. *Int J Adapt Control Signal Process*. 2003;17:625–634.
21. Kano M, Maruta H, Kugemoto H, Shimizu K. Practical model and detection algorithm for valve stiction. In *Proceedings of the IFAC Symposium on Dynamics and Control of Process Systems*. Cambridge, MA, 2004:859–864.
22. He QP, Wang J, Pottmann M, Qin SJ. A curve fitting method for detecting valve stiction in oscillating control loops. *Ind Eng Chem Res*. 2007;46:4549–4560.
23. Feemster M, Vedagarbha P, Dawson DM, Haste D. Adaptive control techniques for friction compensation. In *Proceedings of the American Control Conference*. Philadelphia, PA, 1998:1488–1492.
24. Friedland B, Park Y-J. On adaptive friction compensation. *IEEE Trans Autom Control*. 1992;37:1609–1612.
25. Huang SN, Tan KK, Lee TH. Adaptive friction compensation using neural network approximations. *IEEE Trans Syst Man Cybern C Appl Rev*. 2000;30:551–557.
26. Hägglund T. A friction compensator for pneumatic control valves. *J Process Control*. 2002;12:897–904.
27. Sivagamasundari S, Sivakumar D. A new methodology to compensate stiction in pneumatic control valves. *Int J Soft Comput Eng*. 2013;2:480–484.
28. Coughanowr DR, LeBlanc SE. *Process Systems Analysis and Control*, 3rd ed. Boston, MA: McGraw-Hill, 2009.
29. Ivan LZX, Lakshminarayanan S. A new unified approach to valve stiction quantification and compensation. *Ind Eng Chem Res*. 2009; 48:3474–3483.
30. Jamaludin Z, Van Brussel H, Swevers J. Design of a disturbance observer and model-based friction feedforward to compensate quadrant glitches. In: Ulbrich H, Ginzinger L, editors. *Motion and Vibration Control*. The Netherlands: Springer, 2009:143–153.
31. Cuadros MAdSL, Munaro CJ, Munareto S. Novel model-free approach for stiction compensation in control valves. *Ind Eng Chem Res*. 2012;51:8465–8476.
32. Srinivasan R, Rengaswamy R. Stiction compensation in process control loops: a framework for integrating stiction measure and compensation. *Ind Eng Chem Res*. 2005;44:9164–9174.
33. Srinivasan R, Rengaswamy R. Approaches for efficient stiction compensation in process control valves. *Comput Chem Eng*. 2008;32: 218–229.
34. Cuadros MAdSL, Munaro CJ, Munareto S. Improved stiction compensation in pneumatic control valves. *Comput Chem Eng*. 2012;38: 106–114.
35. Wang J. Closed-loop compensation method for oscillations caused by control valve stiction. *Ind Eng Chem Res*. 2013;52:13006–13019.
36. Gerry J, Ruel M. How to measure and combat valve stiction online. In *Proceedings of the ISA International Fall Conference*. Houston, TX, 2001.
37. Li C, Choudhury MAAS, Huang B, Qian F. Frequency analysis and compensation of valve stiction in cascade control loops. *J Process Control*. 2014;24:1747–1760.
38. Ale Mohammad M, Huang B. Compensation of control valve stiction through controller tuning. *J Process Control*. 2012;22:1800–1819.
39. Cheng C-C, Chen C-Y, Chiu G T-C. Predictive control with enhanced robustness for precision positioning in frictional environment. *IEEE/ASME Trans Mechatronics*. 2002;7:385–392.
40. Hampson SP. Nonlinear Model Predictive Control of a Hydraulic Actuator: Theory and Implementation. PhD Thesis. University of Canterbury, 1995.
41. Su SW, Nguyen H, Jarman R, Zhu J, Lowe D, McLean P, Huang S, Nguyen NT, Nicholson R, Weng K. Model predictive control of a gantry crane with input nonlinearity compensation. In *Proceedings of the World Academy of Science, Engineering and Technology*. Penang, Malaysia, 2009: 312–316.
42. Zabiri H, Samyudia Y. A hybrid formulation and design of model predictive control for systems under actuator saturation and backlash. *J Process Control*. 2006;16:693–709.
43. Zabiri H, Samyudia Y. MIQP-based MPC in the presence of control valve stiction. *Chem Prod Process Model*. 2009;4:85–97.
44. del Carmen Rodríguez Liñán M, Heath WP. MPC for plants subject to saturation and deadzone, backlash or stiction. In *Proceedings of the 4th IFAC Nonlinear Model Predictive Control Conference*. Noorwijkerhout, The Netherlands, 2012:418–423.
45. Durand H, Ellis M, Christofides PD. Integrated design of control actuator layer and economic model predictive control for nonlinear processes. *Ind Eng Chem Res*. 2014;53:20000–20012.
46. Belimo AirControls (USA), Inc. *Electronic Valve Applications Guide*. DOC.V4.2-03.99-7.5M. Available at: http://www.belimo.us/americas/resources.html. Accessed on October 20, 2015.
47. Bishop T, Chapeaux M, Jaffer L, Nair K, Patel S. Ease control valve selection. *Chem Eng Prog*. 2002:52–56.
48. Liptak BG, Boyes WH. Applying control valves. In: Boyes W, editor. *Instrumentation Reference Book*, 4th ed. Boston, MA: Butterworth-Heinemann, 2010:631–636.
49. Darby ML, Nikolaou M, Jones J, Nicholson D. RTO: an overview and assessment of current practice. *J Process Control*. 2011;21:874–884.
50. Christofides PD, El-Farra NH. *Control of Nonlinear and Hybrid Process Systems: Designs for Uncertainty, Constraints and Time-Delays*. Berlin, Germany: Springer-Verlag, 2005.

51. Khalil HK. *Nonlinear Systems*, 3rd ed. Upper Saddle River, NJ: Prentice Hall, 2002.
52. El-Farra NH, Christofides PD. Bounded robust control of constrained multivariable nonlinear processes. *Chem Eng Sci*. 2003;58:3025–3047.
53. Lin Y, Sontag ED. A universal formula for stabilization with bounded controls. *Syst Control Lett*. 1991;16:393–397.
54. Mhaskar P, El-Farra NH, Christofides PD. Stabilization of nonlinear systems with state and control constraints using Lyapunov-based predictive control. *Syst Control Lett*. 2006;55:650–659.
55. Muñoz de la Peña D, Christofides PD. Lyapunov-based model predictive control of nonlinear systems subject to data losses. *IEEE Trans Autom Control*. 2008;53:2076–2089.
56. Qin SJ, Badgwell TA. A survey of industrial model predictive control technology. *Control Eng Pract*. 2003;11:733–764.
57. Heidarinejad M, Liu J, Christofides PD. Economic model predictive control of nonlinear process systems using Lyapunov techniques. *AIChE J*. 2012;58:855–870.
58. Ellis M, Durand H, Christofides PD. A tutorial review of economic model predictive control methods. *J Process Control*. 2014;24:1156–1178.
59. Rawlings JB, Angeli D, Bates CN. Fundamentals of economic model predictive control. In *Proceedings of the 51st IEEE Conference on Decision and Control*. Maui, HI, 2012:3851–3861.
60. Christofides PD, Liu J, Muñoz de la Peña D. *Networked and Distributed Predictive Control: Methods and Nonlinear Process Network Applications. Advances in Industrial Control Series*. London, England: Springer-Verlag, 2011.
61. Amrit R, Rawlings JB, Angeli D. Economic optimization using model predictive control with a terminal cost. *Annu Rev Control*. 2011;35:178–186.
62. Mayne DQ. Control of constrained dynamic systems. *Eur J Control*. 2001;7:87–99.
63. Diehl M, Amrit R, Rawlings JB. A Lyapunov function for economic optimizing model predictive control. *IEEE Trans Autom Control*. 2011;56:703–707.
64. Fagiano L, Teel AR. Generalized terminal state constraint for model predictive control. *Automatica*. 2013;49:2622–2631.
65. Huang R, Biegler LT, Harinath E. Robust stability of economically oriented infinite horizon NMPC that include cyclic processes. *J Process Control*. 2012;22:51–59.
66. Mayne DQ, Rawlings JB, Rao CV, Scokaert POM. Constrained model predictive control: stability and optimality. *Automatica*. 2000; 36:789–814.
67. Ellis M, Durand H, Christofides PD. Elucidation of the role of constraints in economic model predictive control. *Annu Rev Control*. In press.
68. Srinivasan R, Rengaswamy R, Miller R. Control loop performance assessment. 1. A qualitative approach for stiction diagnosis. *Ind Eng Chem Res*. 2005;44:6708–6718.
69. Horch A. *Condition Monitoring of Control Loops*. PhD Thesis. Royal Institute of Technology, 2000.
70. Anderson KL, Blankenship GL, Lebow LG. A rule-based adaptive PID controller. In *Proceedings of the 27th IEEE Conference on Decision and Control*. Austin, TX, 1988:564–569.
71. Leosirikul A, Chilin D, Liu J, Davis JF, Christofides PD. Monitoring and retuning of low-level PID control loops. *Chem Eng Sci*. 2012; 69:287–295.
72. Veronesi M, Visioli A. Performance assessment and retuning of PID controllers for integral processes. *J Process Control*. 2010;20: 261–269.
73. Choudhury MAAS, Shah SL, Thornhill NF, Shook DS. Automatic detection and quantification of stiction in control valves. *Control Eng Pract*. 2006;14:1395–1412.
74. Lee KH, Ren Z, Huang B. Novel closed-loop stiction detection and quantification method via system identification. In *Proceedings of the International Symposium on Advanced Control of Industrial Processes*. Jasper, Canada, 2008.
75. Lao L, Ellis M, Christofides PD. Smart manufacturing: handling preventive actuator maintenance and economics using model predictive control. *AIChE J*. 2014;60:2179–2196.
76. Mhaskar P, Kennedy AB. Robust model predictive control of nonlinear process systems: handling rate constraints. *Chem Eng Sci*. 2008; 63:366–375.
77. Mhaskar P, Liu J, Christofides PD. *Fault-Tolerant Process Control: Methods and Applications*. London, England: Springer-Verlag, 2013.
78. Özgülşen F, Adomaitis RA, Çinar A. A numerical method for determining optimal parameter values in forced periodic operation. *Chem Eng Sci*. 1992;47:605–613.
79. Alfani F, Carberry JJ. An exploratory kinetic study of ethylene oxidation over an unmoderated supported silver catalyst. *Chim Ind*. 1970;52:1192–1196.
80. Romanenko A, Santos LO, Afonso PAFNA. Application of agent technology concepts to the design of a fault-tolerant control system. *Control Eng Pract*. 2007;15:459–469.
81. Ellis M, Christofides PD. Real-time economic model predictive control of nonlinear process systems. *AIChE J*. 2015;61:555–571.
82. Wächter A, Biegler LT. On the implementation of an interior-point filter line-search algorithm for large-scale nonlinear programming. *Math Program*. 2006;106:25–57.

*Manuscript received Oct. 27, 2015, and revision received Jan. 8, 2016.*